

Living and Dead foraminiferal assemblages of the last decades from Kveithola Trough: taphonomic processes and ecological highlights.

Highlights

Monitoring recent short and long-term climatic variations in the Kveithola Trough.

Comparison of the living and dead foraminiferal assemblages

Integration of the foraminifera, oceanographic and sedimentological data.

Analysis of taphonomic processes using the living and dead foraminiferal assemblages

Evaluation of bias on the paleocological reconstruction due to taphonomy

Living and Dead foraminiferal assemblages of the last decades from Kveithola Trough:
taphonomic processes and ecological highlights.

Viviana Maria Gamboa Sojo ^{a,b,c}, Katrine Husum ^d, Francesca Caridi ^e, Renata G. Lucchi ^{f,g}, Manuel Bensi ^f,
Vedrana Kovacevic ^f, Anna Sabbatini ^e, Leonardo Langone ^h, Aleksander Tadeusz Dominiczak ⁱ, Patricia
Povea ^j, Caterina Morigi ^{a,k}

- a. Department of Earth Sciences. University of Pisa, Pisa, Italy
- b. Department of Earth Sciences. University of Florence, Florence, Italy
- c. Department of Earth Sciences. University of Costa Rica, San Jose Costa Rica
- d. NPI Norwegian Polar Institute, Fram Centre, Tromsø, Norway
- e. Department of Life and Environmental Sciences, Polytechnic University of Marche, Ancona, Italy
- f. National Institute of Oceanography and Applied Geophysics (OGS), Trieste, Italy.
- g. Centre for Arctic Gas Hydrate, Environment and Climate (CAGE), UiT-The Arctic University of
Norway, Tromsø, Norway
- h. Institute of Polar Sciences, Italian National Research Council (CNR-ISP), Bologna, Italy
- i. Institute of Geology, Adam Mickiewicz University in Poznan, Poland
- j. University of Barcelona, Barcelona Spain
- k. Stratigraphy Department, Geological Survey of Denmark and Greenland (GEUS), Copenhagen,
Denmark

1
2
3
4
5 Living and Dead foraminiferal assemblages of the last decades from Kveithola Trough:
6
7
8 taphonomic processes and ecological highlights.
9

10
11
12
13 Abstract

14
15
16
17 We examine the living and dead benthic foraminiferal assemblages from the topmost 10cm (using
18
19 150 μm sieve fraction) of three sedimentological short records collected in the Kveithola Trough
20
21 (northwest Barents Sea). Our aim is to reconstruct the environmental variations of the last decades,
22
23 connected to the interaction among the North Atlantic and the Arctic water masses. Our samples
24
25 are collected at water depths between 150 and 380 m during the Eurofleets2-BURSTER
26
27 oceanographic cruise, on board of the R/V Polarstern (June 2016).

28
29
30 In the Cell Tracker Green (CTG) labelled living foraminiferal fauna, the main species are *Pullenia bulloides*,
31
32 *Globobulimina auriculata*, and *Nonionellina labradorica*, while in the dead assemblages the main species
33
34 are *Cassidulina neoteretis*, *Cibicidoides lobatulus*, and *Cassidulina reniforme* (outer, inner, and shelf
35
36 stations, respectively). The dead foraminiferal assemblages show no significant traceable environmental
37
38 changes in the Kveithola Trough area occurred during the last *ca.* 100 years. Conversely, the living
39
40 foraminiferal fauna shows that this area is subject to variations related to circulation changes and organic
41
42 matter burial in sediments, to which the biota adapts quickly. Moreover, the species that are only
43
44 observed in the dead foraminiferal assemblages and not in the living CTG-labelled foraminiferal
45
46 assemblages (e.g. *C. reniforme*) are typical of colder water and highlight the ongoing warming of the Arctic
47
48 area. We find that the preservation of foraminiferal tests may bias the paleontological results. The
49
50 agglutinated tests are often disintegrated, and the delicate calcareous ones are broken. The
51
52 environmental conditions (style of sedimentation, bottom currents, interaction with other communities)
53
54
55
56
57
58
59
60 can weaken the foraminiferal tests and make them prone to breakage or dissolution.
61
62
63
64
65

1
2
3
4
5
6
7
8
9
10
11
12
13
14
15
16
17
18
19
20
21
22
23
24
25
26
27
28
29
30
31
32
33
34
35
36
37
38
39
40
41
42
43
44
45
46
47
48
49
50
51
52
53
54
55
56
57
58
59
60
61
62
63
64
65

Keywords Living vs. dead benthic foraminifera; taphonomic processes; oceanographic processes;

Kveithola Trough (Barents Sea); Arctic.

1
2
3
4
5 Living and Dead foraminiferal assemblages of the last decades from Kveithola Trough:
6
7
8 taphonomic processes and ecological highlights.
9

10
11 Viviana Maria Gamboa Sojo ^{a.b.c.}, Katrine Husum ^{d.}, Francesca Caridi ^{e.}, Renata G. Lucchi ^{f.g.}, Manuel Bensi ^{f.},
12
13
14 Vedrana Kovacevic ^{f.}, Anna Sabbatini ^{e.}, Leonardo Langone ^{h.}, Aleksander Tadeusz Dominiczak ^{i.}, Patricia
15
16 Povea ^{j.}, Caterina Morigi ^{a.k.}

- 17
18
19 a. Department of Earth Sciences. University of Pisa, Pisa, Italy
20
21 b. Department of Earth Sciences. University of Florence, Florence, Italy
22
23
24 c. Department of Earth Sciences. University of Costa Rica, San Jose Costa Rica
25
26 d. NPI Norwegian Polar Institute, Fram Centre, Tromsø, Norway
27
28
29 e. Department of Life and Environmental Sciences, Polytechnic University of Marche, Ancona, Italy
30
31 f. National Institute of Oceanography and Applied Geophysics (OGS), Trieste, Italy.
32
33
34 g. Centre for Arctic Gas Hydrate, Environment and Climate (CAGE), UiT-The Arctic University of
35
36 Norway, Tromsø, Norway
37
38 h. Institute of Polar Sciences, Italian National Research Council (CNR-ISP), Bologna, Italy
39
40
41 i. Institute of Geology, Adam Mickiewicz University in Poznan, Poland
42
43 j. University of Barcelona, Barcelona Spain
44
45 k. Stratigraphy Department, Geological Survey of Denmark and Greenland (GEUS), Copenhagen,
46
47
48 Denmark

49
50
51 Corresponding authors: Viviana Maria Gamboa Sojo, Caterina Morigi

52
53
54 E-mail address: vivianamaria.gamboasojo@unifi.it, caterina.morigi@unipi.it
55
56
57
58
59
60
61
62
63
64
65

1
2
3
4 Abstract
5
6
7

8 We examine the living and dead benthic foraminiferal assemblages from the topmost 10cm (using
9
10 150 µm sieve fraction) of three sedimentological short records collected in the Kveithola Trough
11
12 (northwest Barents Sea). Our aim is to reconstruct the environmental variations of the last decades,
13
14 connected to the interaction among the North Atlantic and the Arctic water masses. Our samples
15
16 are collected at water depths between 150 and 380 m during the Eurofleets2-BURSTER
17
18 oceanographic cruise, on board of the R/V Polarstern (June 2016).
19

20
21
22 In the Cell Tracker Green (CTG) labelled living foraminiferal fauna, the main species are *Pullenia bulloides*,
23
24 *Globobulimina auriculata*, and *Nonionellina labradorica*, while in the dead assemblages the main species
25
26 are *Cassidulina neoteretis*, *Cibicidoides lobatulus*, and *Cassidulina reniforme* (outer, inner, and shelf
27
28 stations, respectively). The dead foraminiferal assemblages show no significant traceable environmental
29
30 changes in the Kveithola Trough area occurred during the last ca. 100 years. Conversely, the living
31
32 foraminiferal fauna shows that this area is subject to variations related to circulation changes and organic
33
34 matter burial in sediments, to which the biota adapts quickly. Moreover, the species that are only
35
36 observed in the dead foraminiferal assemblages and not in the living CTG-labelled foraminiferal
37
38 assemblages (e.g. *C. reniforme*) are typical of colder water and highlight the ongoing warming of the Arctic
39
40 area. We find that the preservation of foraminiferal tests may bias the paleontological results. The
41
42 agglutinated tests are often disintegrated, and the delicate calcareous ones are broken. The
43
44 environmental conditions (style of sedimentation, bottom currents, interaction with other communities)
45
46 can weaken the foraminiferal tests and make them prone to breakage or dissolution.
47
48
49
50
51

52
53
54
55 **Keywords** Living vs. dead benthic foraminifera; taphonomic processes; oceanographic processes;
56
57 Kveithola Trough (Barents Sea); Arctic.
58
59
60
61
62
63
64
65

1
2
3
4 1. Introduction.
5
6
7

8 Polar regions are extremely sensitive areas to long-term climatic variations, which include both natural
9
10 and anthropogenic influences. As indicated in the IPCC (Intergovernmental Panel on Climate Change) 2019
11
12 report, these changes include variations in the Arctic temperature and sea ice extent, producing
13
14 alterations in the ocean salinity and primary production, and extreme weather conditions around the
15
16 world (precipitations, droughts, heat, and cyclones; Solomon et al., 2007). The sea ice extent and the
17
18 seasonal/interannual variations of temperature, albedo, productivity, etc., principally influence the Arctic
19
20 Ocean (Serreze et al., 2007; Screen and Simmonds, 2010a; Comiso and Hall, 2014; Lind et al., 2018). The
21
22 marginal Barents Sea is located south of this area and is characterised by two main climatic regions, the
23
24 cold sea ice covered area in the north and the warmer and productive area in the south (Loeng, 1991;
25
26 Screen and Simmonds, 2010b; Smedsrud et al., 2013; Lind et al., 2018).
27
28
29

30
31
32
33 The Kveithola glacial trough system in the NW Barents Sea corresponds to a complex geomorphological
34
35 environment located at the sea ice limit and influenced by the interaction of different water masses
36
37 (Atlantic and Arctic waters) (Aagaard, 1989; Loeng, 1991; Vinje and Kvambekk, 1991; Loeng et al., 1997;
38
39 Orvik and Niiler, 2002; Maslowski et al., 2004; Smedsrud et al., 2013). Quaternary climate studies of the
40
41 Barents Sea, based on sedimentary data set, indicate a general increase in the sea temperature (Duplessy
42
43 et al., 2001; Rebesco et al., 2011; R  ther et al., 2012; Groot et al., 2014; Dijkstra et al., 2017a). In particular,
44
45 some papers highlighted the variation in the inflow of the warm Atlantic water into the Barents Sea during
46
47 the Holocene (Duplessy et al., 2001; Sarnthein et al., 2003;   lubowska-Woldengen et al., 2007; Groot et
48
49 al., 2014).
50
51
52

53
54
55
56 Some of these paleoclimatic studies have been based on benthic foraminiferal records from the Barents
57
58 Sea (e.g. Sarnthein et al., 2003;   lubowska-Woldengen et al, 2007; Groot et al., 2014; Dijkstra et al.,
59
60
61

1
2
3
4 2017a). Benthic foraminifera are important (paleo-) ecological indicators due to their wide diffusion in the
5
6
7 oceans, and their good potential preservation in the fossil record. The distribution of the foraminiferal
8
9 living assemblages in the Barents Sea is strongly related to water mass characteristics, e.g. temperature
10
11 and available nutrition (e.g. Saher et al., 2012; Dijkstra et al., 2013). Studies that compare the living and
12
13 dead benthic foraminiferal assemblages point to some preservation issues (transport, bioturbation,
14
15 dissolution and/or broken test), which may bias the interpretation of the fossil record (e.g., Hald and
16
17 Korsun, 1997; Wollenburg and Mackensen, 1998; Dijkstra et al., 2017a; Dijkstra et al., 2017b).
18
19

20
21
22 Based on this premise, the objective of this study is threefold: 1) to discuss the distribution of living
23
24 foraminiferal assemblages in the Kveithola Trough and their relation to the local oceanographic processes;
25
26
27 2) to evaluate the taphonomic processes that bias the ecological interpretation in a high-latitude
28
29 environment; and 3) to reconstruct environmental variations of the last decades on the basis of the dead
30
31 foraminiferal assemblages. To reach these objectives we have analysed oceanographic,
32
33 geomorphological, and sedimentological data as potential drivers of the living and dead foraminiferal
34
35 assemblages.
36

37 38 39 40 41 42 43 44 2. Bathymetric features and oceanographic patterns of the study area

45
46
47
48 The Kveithola Trough located in the NW Barents Sea, is an abrupt bathymetric feature about 100 km long
49
50 and 13 km wide, with a water depth ranging from 100 to 400 m (Fohrmann et al., 1998; R  ther et al., 2012)
51
52 (Fig. 1). The longitudinal profile of the trough is markedly staircase-like, composed of five transverse ridges
53
54 located about 15 km apart from each other, and interpreted as Grounding Zone Wedges (*sensu*
55
56 Dowdeswell and Fugelli, 2012) that testify the episodic mode of the retreat of former ice stream(s) after
57
58 Last Glacial Maximum (Rebesco et al., 2011; Bjarnad  ttir et al., 2013). Other prominent seafloor
59
60
61
62
63
64
65

1
2
3
4 morphological features are mega-scale glacial lineations generated by grounded ice sheet advance
5
6
7 (Rebesco et al., 2011), and two mounded depocentres with an associated moat developing along the
8
9 northern margin of the glacial trough that are interpreted as a sediment drift complex (Rebesco et al.,
10
11 2016) (Fig. 1). The northernmost area is crossed by a pronounced moat, that channelize dense bottom
12
13 currents crossing the trough from the inner (East) to the outer (West) area delivering sediments to the
14
15 shelf break and to the drift system (Rebesco et al., 2016; Lantzsch et al., 2017) (Fig. 1). Another important
16
17 element in the area is a system of faults in the inner part of the Kveithola Trough and the northern part
18
19 of the shelf evidenced by Mau et al. (2017). Along this fault system a local evidence of hydrocarbon
20
21 seepage activity is detected (station 21) (Lucchi et al., 2016; Mau et al., 2017; Bazzaro et al., 2020), driving
22
23
24
25
26
27
28
29
30
31
32
33
34
35
36
37
38
39
40
41
42
43
44
45
46
47
48
49
50
51
52
53
54
55
56
57
58
59
60
61
62
63
64
65

macrofaunal diversity and trophic conditions (Caridi et al., 2019).

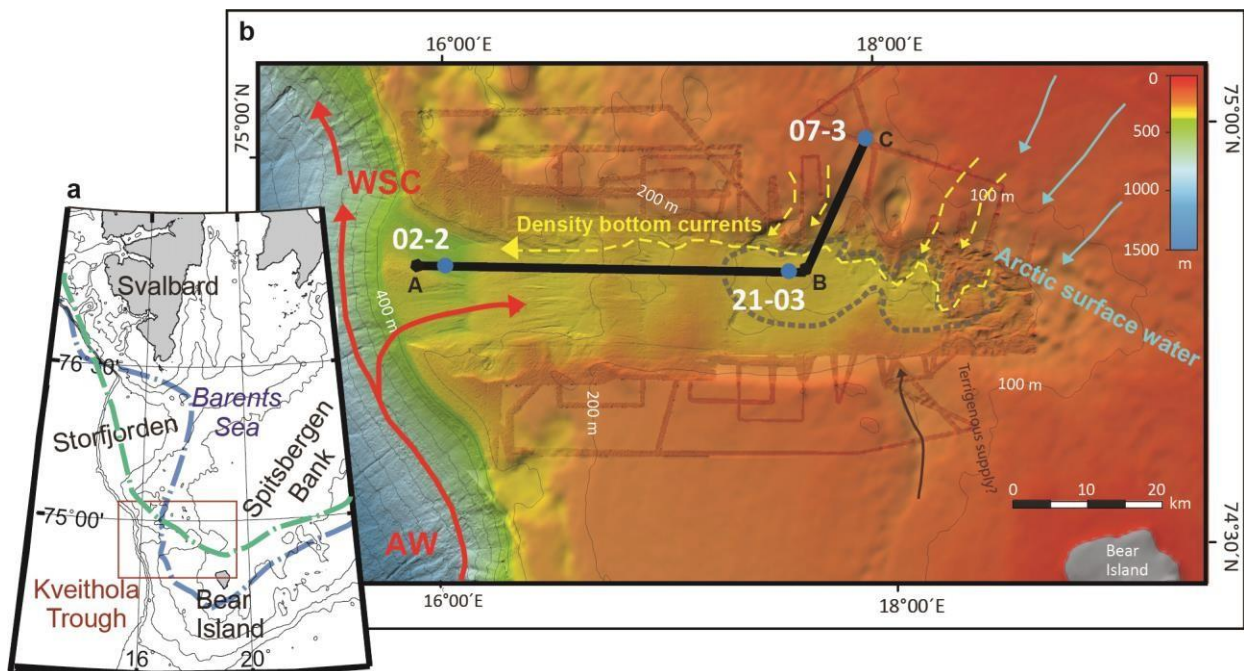


Fig. 1. (a) Overview map showing the location of the Kveithola Trough in the NW Barents Sea. The blue
dot-dashed line shows the position of the Polar Front (Harris et al., 1998). The green dot-dashed line

1
2
3
4 represents the mean of the maximum sea ice extent from 1980-2010 (National Snow and Ice Data Centre
5
6
7 (NSIDC, <https://nsidc.org/>). (b) Bathymetric map of Kveithola Trough. The black ABC line shows the
8
9 location of the bathymetric profile displayed in Fig. 7. The blue filled circles indicate the cored sites. The
10
11 red arrows represent the path of the West Spitsbergen Current (WSC), whereas the light blue arrows
12
13 indicate the input of the Arctic surface water. The yellow dashed arrows indicate the direction of density
14
15 bottom currents. The grey dashed polygon on the inner Kveithola Trough delimits the sediment drift
16
17 complex, and the dark brown arrow indicates a possible terrigenous supply coming from the south
18
19 (Lantzsch et al., 2017).
20
21
22
23
24
25
26
27

28 Relatively fresh, cold Arctic waters (ArW) and warm, salty Atlantic waters (AW) constantly interact within
29
30 the Kveithola Trough (Fig. 1). ArW flow from the Arctic Ocean and influence the northern-eastern part of
31
32 the trough (Aagaard et al., 1985; Aagaard, 1989; Loeng, 1991; Orvik and Niiler, 2002); whereas the warm
33
34 and saline AW are transported in the area by the West Spitsbergen Current (WSC), representing the
35
36 northernmost branch of the North Atlantic Current proceeding from south along the bathymetric contour
37
38 (Aagaard et al., 1973; Aagaard et al., 1981; Aagaard, 1989; Vinje and Kvambekk, 1991; Loeng et al., 1997;
39
40 Maslowski et al., 2004; Smedsrud et al., 2013). The Kveithola Trough is seasonally influenced by the
41
42 presence of sea ice during the winter seasons as it is on the southern limit of the maximum ice extent
43
44 during late winter, around March-April (Fig. 1). However, the sea-ice extent in the Barents Sea suffers
45
46 from a strong interannual variability as well as a progressive long-term reduction (www.mosj.no). Decadal
47
48 oscillations of the sea-ice extent in the Arctic and hence in the Barents Sea seem to be linked to large scale
49
50 climatic patterns such as the Pacific Decadal Oscillation, the North Pacific Gyre Oscillation, and the North
51
52 Atlantic Oscillation-like atmospheric pressure conditions (see e.g., Koenigk et al., 2009; Yang et al., 2020).
53
54
55
56
57
58
59
60
61
62
63
64
65

3. Materials and methods

The geological and oceanographic dataset presented in this work was collected during the Eurofleets 2- BURSTER cruise on-board the R/V Polarstern (Expedition PS99-1a), Bremerhaven-Longyearbyen, June 13– 23, 2016 (Lucchi et al., 2016). The data were acquired over the Kveithola area between 19th and 20th June 2016.

3.1 Oceanographic data set

3.1.1 Thermohaline data

Temperature (T, °C), salinity (SAL, PSU) and dissolved oxygen (DO, ml l⁻¹), were recorded throughout the water column by means of a SeaBird 911-plus CTD (Conductivity-Temperature-Depth) mounted on the SBE 32 Carousel Water Sampler (Rosette) equipped with 24 Niskin Bottles (12-liter capacity). The DO concentration was also determined in parallel on water samples taken at discrete depths from the Niskin bottles using the Winkler method (Carpenter, 1965).

Potential temperature (θ , °C) was calculated from each original in-situ data set using the toolbox TEOS-10 (<http://www.teos-10.org/software.htm>). Some data were plotted using Ocean Data View (ODV; Schlitzer, 2021).

3.1.2 Horizontal currents

The vertical distributions of horizontal currents were obtained from a vessel mounted Acoustic Doppler Current Profiler (vmADCP, Teledyne RDI 150 kHz Ocean Surveyor configured in 'Narrowband' mode). The water column was divided into 80 cells with 4 m size obtaining data in the range from approximately 10 m to 320 m depth. However, the vmADCP cannot sample more than 80–90 % of the water column within its

1
2
3
4 operating range, so it does not allow for measuring currents close to the seafloor. In our study area, the
5
6 blanking distance amounts to about 40-50 m above the seafloor.
7
8

9 10 *3.1.3 Satellite images*

11
12 To identify the southern limit of the sea ice extent during winter, we used satellite images that are freely
13
14 available from the NASA Worldview application (<https://worldview.earthdata.nasa.gov>), part of the NASA
15
16 Earth Observing System Data, and Information System (EOSDIS). The spatial imagery resolution is 250 m,
17
18 and the temporal resolution is daily.
19
20
21
22
23
24

25 3.2 Geological data set

26
27 Multicore samples were collected using a video-guided multi-corer (TV-MUC), along a west- east
28
29 (outer- inner) transect in the Kveithola Trough, at water depths ranging from 376 m to 159 m (Fig. 1;
30
31 Tab. 1). Two cores from each deployment were selected. One core was sampled on-board for living
32
33 benthic foraminiferal analysis, and a second core was opened, described, subsampled on-board and used
34
35 for radiometric dating and analysis of grain size and dead benthic foraminifera. In this study, we focus on
36
37 the upper 10 cm of the sediment cores, which were sliced at every 0.5 cm for the upper 2 cm and at every
38
39 1 cm in the interval between 2-10 cm below seafloor (bsf).
40
41
42
43
44
45
46
47
48
49
50
51
52
53
54
55
56
57
58
59
60
61
62
63
64
65

1
2
3
4 Tab. 1. Location and water depth of the multi-cores, and average values (0-10 cm bsf) of physical and
5
6
7 biochemical characteristics. BAC = bioavailable carbon, and algal fraction of BPC, Lipid and CHO =
8
9 carbohydrates (from Caridi et al., 2019).

10
11
12
13

Station	Coordinates	Water depth (m)	Mean grain size (phi)	BAC (mg/g)	Algal fraction of bpc%	Lipid (mg/g)	CHO (mg/g)
02	74° 51.49' N, 16° 05.84' E	376	4	2.52	10.45	0.49	2.34
21	74° 52.40' N; 17° 21.60' E	306	5	6.23	17.27	1.27	7.00
07	4° 59.69' N; 17° 59.72' E	159	6	5.97	34.13	1.72	7.02

14
15
16
17
18
19
20
21
22 *3.2.1 Grain size analyses*

23
24
25 Grain size analyses were performed using a Coulter-counter laser Beckman LS-230 scanning the 0.04-
26
27 2000 µm fraction with 0.004 µm resolution. The sediments were treated with peroxide water to eliminate
28 the organic matter, and the disaggregated sediments were suspended into a 0.1% sodium-
29 hexametaphosphate solution to prevent sediment flocculation. The samples were left 3 minutes into an
30 ultrasonic bath prior to measurement. The results were classified according to Friedman and Sanders
31 (1978) grain-size scale.
32
33
34
35
36
37
38
39
40

41 *3.2.2 ²¹⁰Pb and ¹³⁷Cs analysis*

42
43
44 Sedimentation rate (SR) for the three cores was determined on the basis of short-lived radionuclides (²¹⁰Pb
45 and ¹³⁷Cs). Samples of 20 gram of sediment were homogenised, packed in vials of uniform geometry and
46 left for three weeks before they were measured for 24 h with a high-purity germanium detector (Canberra
47 BE3830). The ages and SR were calculated on the basis of constant flux-constant sedimentation model
48 (CF-CS) (Robbins and Edgington, 1975), and the best-fit linear regression was applied to the core region
49 with more regularly decreasing activity, thus discarding data from the surface mixed layer or from
50
51
52
53
54
55
56
57
58
59
60
61
62
63
64
65

1
2
3
4 subsurface peaks. Identification of peaks in ^{137}Cs activity helped to support the depth-age modelling
5
6
7 (Ritchie and McHenry, 1990; Pittauerová, 2013).
8

9 10 3.2.3 *Living and Dead foraminiferal data*

11
12
13
14 For the living foraminiferal analysis, the sediment slices were incubated in a refrigerator for 12-15 hours
15
16 in Cell Tracker Green CMFDA (CTG), and then fixed in 10% formalin buffered with sodium borate solution,
17
18
19 following the staining procedure as indicated in Pucci et al. (2009). CTG is a non-terminal, non-fluorescent
20
21 probe that can be cleaved by non-specific esterase common to living cells, producing a fluorescent
22
23 compound, fluorescein, visible using a fluorescent microscope. The requirement of esterase activity
24
25
26 means that a cell must be alive to produce fluorescence (Bernhard et al., 2006). In the laboratory, the
27
28 sediment samples were sieved through 63, 150 and 500 μm mesh, and kept wet while the whole amount
29
30
31 of living specimens were hand-sorted in water using a fluorescence binocular microscope from both size
32
33 fractions. For this study, we used the data obtained from the coarse fraction (up to 150 μm), besides we
34
35 did not consider the soft-shelled foraminifera because these taxa are not preserved in the
36
37 thanatocoenosis, as their organic tests degrade and disappear as soon as they die. The soft-shelled
38
39 foraminifera were counted only in the living microfauna, found to constitute about the 35% of the total
40
41 living assemblages. Such data set will be discussed in a future study focused on the ecology of soft-shelled
42
43 taxa (Caridi et al., in preparation). To compare living to dead foraminiferal data, we normalised the values
44
45 of the living foraminifera for volume of sediment, in gram of sediment, using the following formula:
46
47
48
49
50

51 $m=\rho V$ where: m = mass of the sediment in gram, ρ = density in g/c.c. and V = volume in c.c.
52

53
54 The samples for analysis of dead foraminiferal assemblages were dry-weighed and wet-sieved using the
55
56
57 mesh size of 63 μm . The sample was then dry-sieved at 150 and 500 μm and analysed for the dead benthic
58
59 **foraminiferal assemblages, while the finer size fractions (63-150 μm) were stored for future studies. At**
60
61

1
2
3
4 least 300 specimens were picked and identified at species level. For each sample, both living and dead
5
6
7 foraminifera were mounted on Plummer cells. The identification at the species level was performed
8
9 following the taxonomy by Ellis and Messina (1940-1978), Loeblich and Tappan (1953, 1988), Feyling-
10
11 Hanssen et al. (1971), Wollenburg and Mackensen (1998) and Holbourn et al. (2013). Eventually, some
12
13 species with similar ecological preferences and belonging to the same genus were grouped together. We
14
15 identified *Buccella frigida* and *Buccella inusitata*, grouped as *Buccella* spp.; *Islandiella norcrossi* and
16
17 *Islandiella helenae*, grouped as *Islandiella* spp.; *Reophax scorpiurus* and *Reophax fusiformis*, grouped as
18
19 *Reophax* spp. Rotaliida spp. comprises a group of species belonging to the same order that we have not
20
21 been able to identify, since their apertural areas are broken making further identification impossible
22
23
24
25
26 (Plate 2). The agglutinated broken tests do not allow the identification at the species level and in some
27
28 cases preclude their recognition at the genus level (Plate 2). The degree of damage of a test or the
29
30 percentage of broken agglutinated tests was not possible to quantify. No further identification was
31
32 attempted, as it is not possible to recognise one individual test by the number of broken pieces found in
33
34 a sample (De Stigter et al., 1999). Species with a relative abundance $\geq 5\%$ in the dead and living
35
36 assemblages are considered as main species.
37

38
39
40
41 Living and dead ratios were calculated to compare the living and dead proportions of species (Jorissen
42
43 and Wittling, 1999; Duros et al; 2012; Dessandier et al, 2018):

44
45
46
47 $l/(l+d)$ where: l = % of living foraminifera and d = % of dead foraminifera
48
49
50

51 The diversity indices, number of species (S), dominance (D) and Shannon (H) index, were calculated using
52
53 the software PAST (Hammer et al., 2001).
54
55
56
57
58
59
60
61
62
63
64
65

4. Results

4.1 Water masses properties and ocean current variability

The horizontal and vertical distribution of the physical and biogeochemical properties have been investigated along four N-S oriented sections, two of which went through (or close to) the stations where the sediment samples were collected and hence are presented here (Fig. 2). We have distinguished two main water masses in the Kveithola Basin in June 2016. The relatively warm and saline AW with $\theta > 4.50$ °C and SAL > 35.10 and colder and fresher water originating from the Barents Sea and the northern shelves with $\theta < 4.00$ °C and SAL < 35.00. Dissolved oxygen (DO) ranges from 4 to 7 ml/l in the study area. The lower DO values are primarily associated with the AW and higher values with the shelf waters (Fig. 2).

Generally, potential temperature salinity are higher in the upper layers with the values 4.00 - 6.95 °C and 34.80 - 35.15 (Fig. 2). Below 200 m water depth there is a core of cold (<4.00 °C), fresh (minimum *ca.* 34.90) and oxygenated water. The outermost S-N transect (S1) is characterised by a more evident AW signal, than the inner transect S3. Along the transect S3, passing near station 21 and above station 07, the frontal separation between AW and shelf waters become sharper, and shelf waters extend from the surface down to the bottom in the northern part of the section (Fig. 2). The near-bottom distributions of potential temperature and salinity reveal higher values (4.30–5.00 °C and 35.03–35.10) in the southern deep part of the study region than in the northern part (Fig. 3). The concentrations of DO are in contrast higher in the north-eastern part of Kveithola.

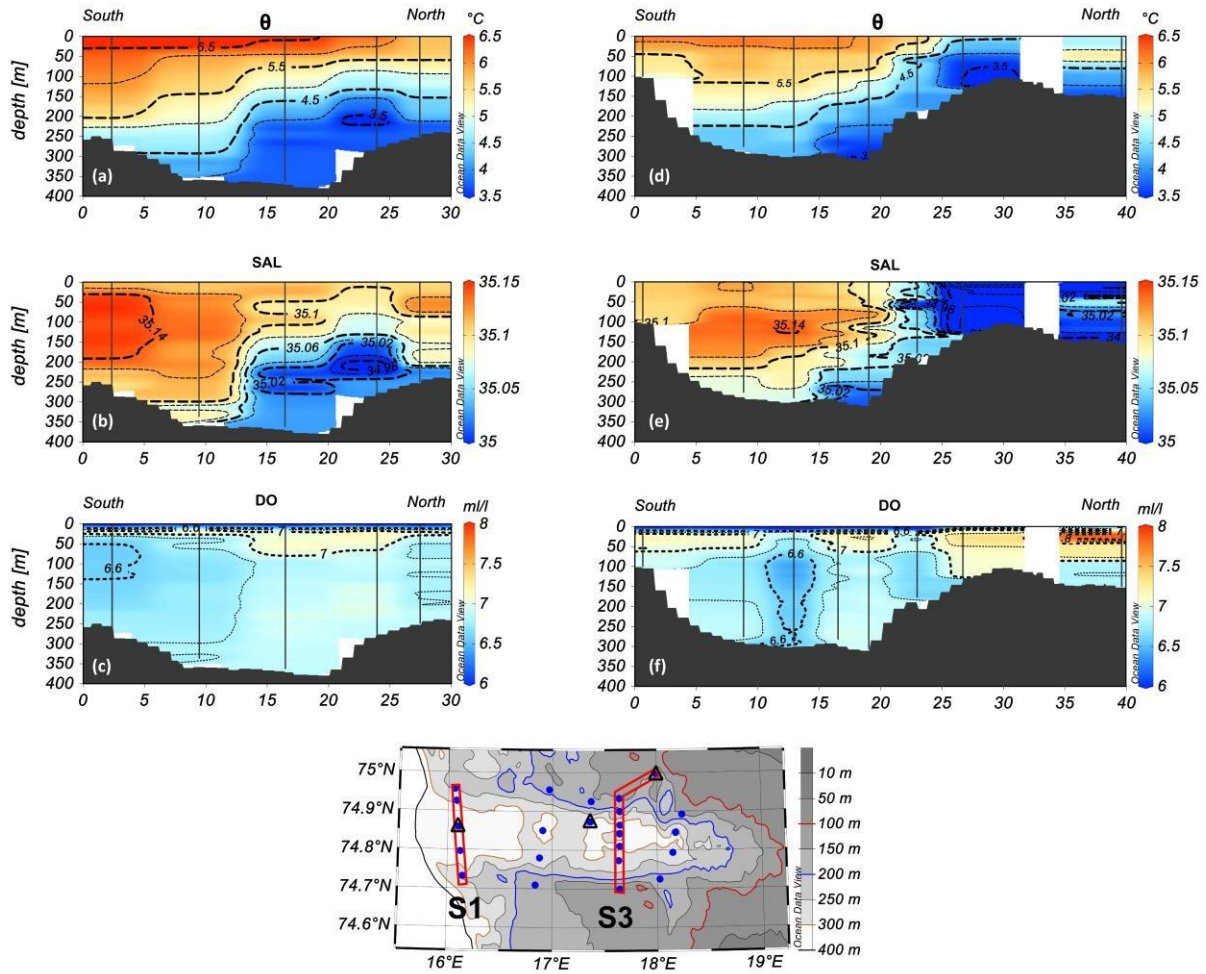


Fig. 2. Vertical distribution of potential temperature θ ($^{\circ}\text{C}$), salinity (SAL) and dissolved oxygen DO (ml/l), along south- north sections S1 (a, b, c) and S3 (d, e, f). The blue filled circles in the sections S1 and S3 indicate the oceanographic stations, while triangles indicate the MUC stations.

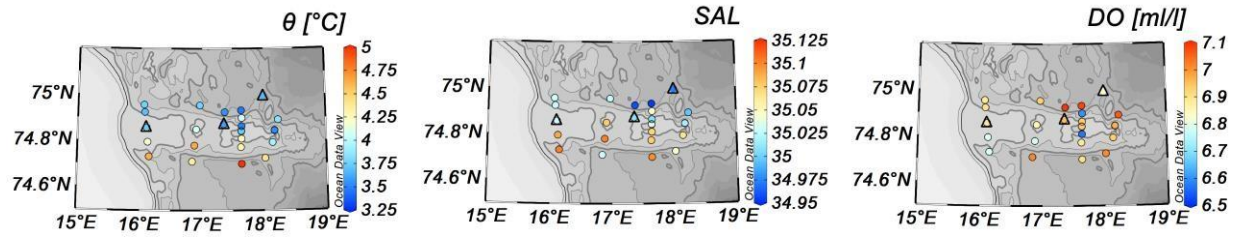
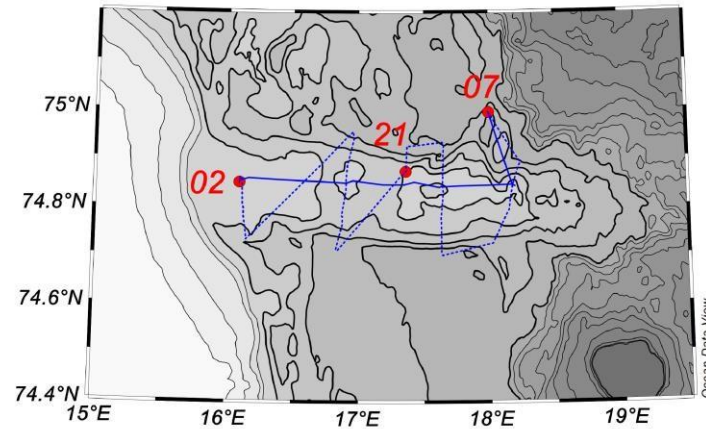


Fig. 3. Near bottom values of potential temperature θ ($^{\circ}\text{C}$), salinity SAL, and dissolved oxygen DO (ml/l), from the CTD data. The triangles indicate the position of the MUC stations used in this work.

The current speed has been measured through most of the water column along the ship's route (Fig. 4a), and it vary between nearly 0 and 0.4 m/s (Fig. 4b). Highest values are recorded between 150 and 200 m water depth near the western border of the Kveithola Trough. Current speeds are low and not exceeding 0.09 m/s in the deeper parts of the water column, while high values are found over areas with the shallower depths within Kveithola.

1
2
3
4
5
6
7
8
9
10
11
12
13
14
15
16
17
18
19
20
21
22
23
24
25
26
27
28
29
30
31
32
33
34
35
36
37
38
39
40
41
42
43
44
45
46
47
48
49
50
51
52
53
54
55
56
57
58
59
60
61
62
63
64
65

(a)



(b)

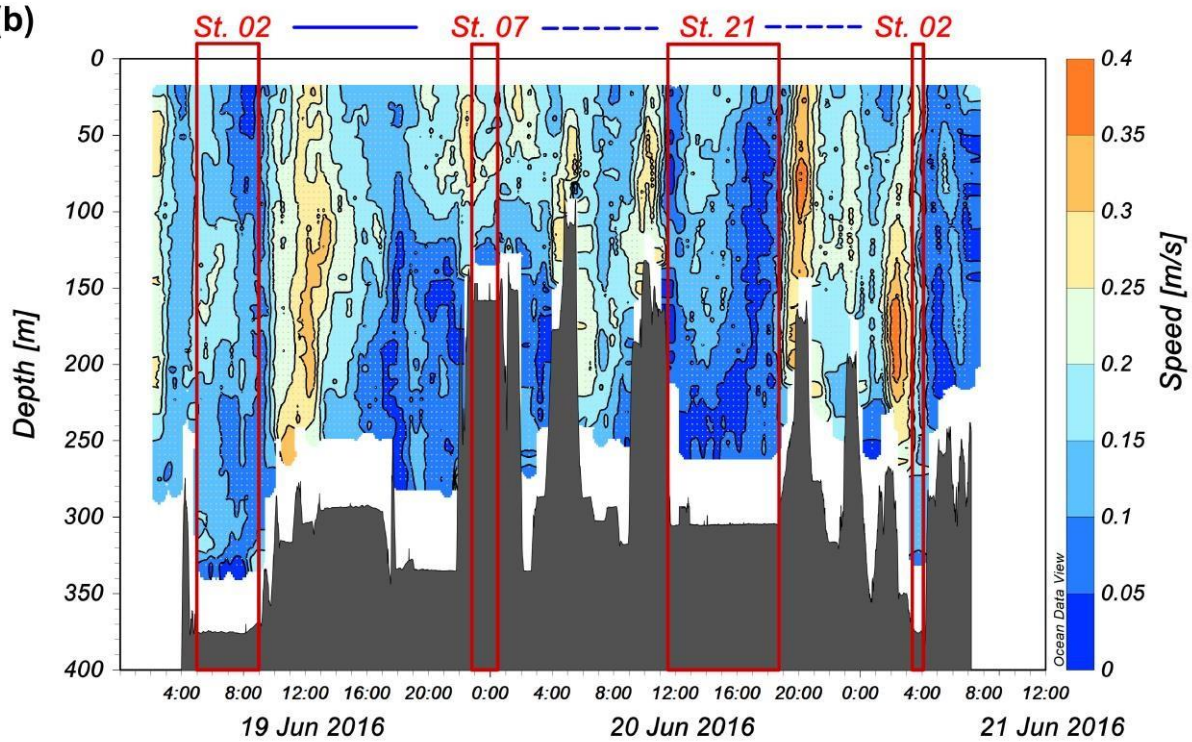


Fig. 4. Current speed the Kveithola Trough. (a) The red filled circles show the location of the three MUC stations (02, 07, and 21) and the track of the ship's route (blue solid line: from St. 02 to St. 07, blue dashed line: from St. 07 towards Sts. 21 and 02). (b) Time-depth diagram of current speed. Station 02 has been surveyed at the beginning and at the end of the cruise.

4.2 Sea ice extension

The maximum seasonal sea ice extent in the Barents Sea usually occurs between March and April. Winter 2016 has been characterised by the lowest sea ice extent during the last 40 years (NSIDC, <https://nsidc.org/>), and little sea ice has been observed in the study area (Fig. 5). In recent years, this area of the Arctic has often been characterised by the absence of ice during the winter period (e.g., Peng et al., 2018). One has to go back to winter 2013 to find sea ice throughout the north-western basin of the Barents Sea, even near the Kveithola Trough (Fig. 5), while the last above-average value for the period 1979-2019 has been recorded in 1998 and 2003.

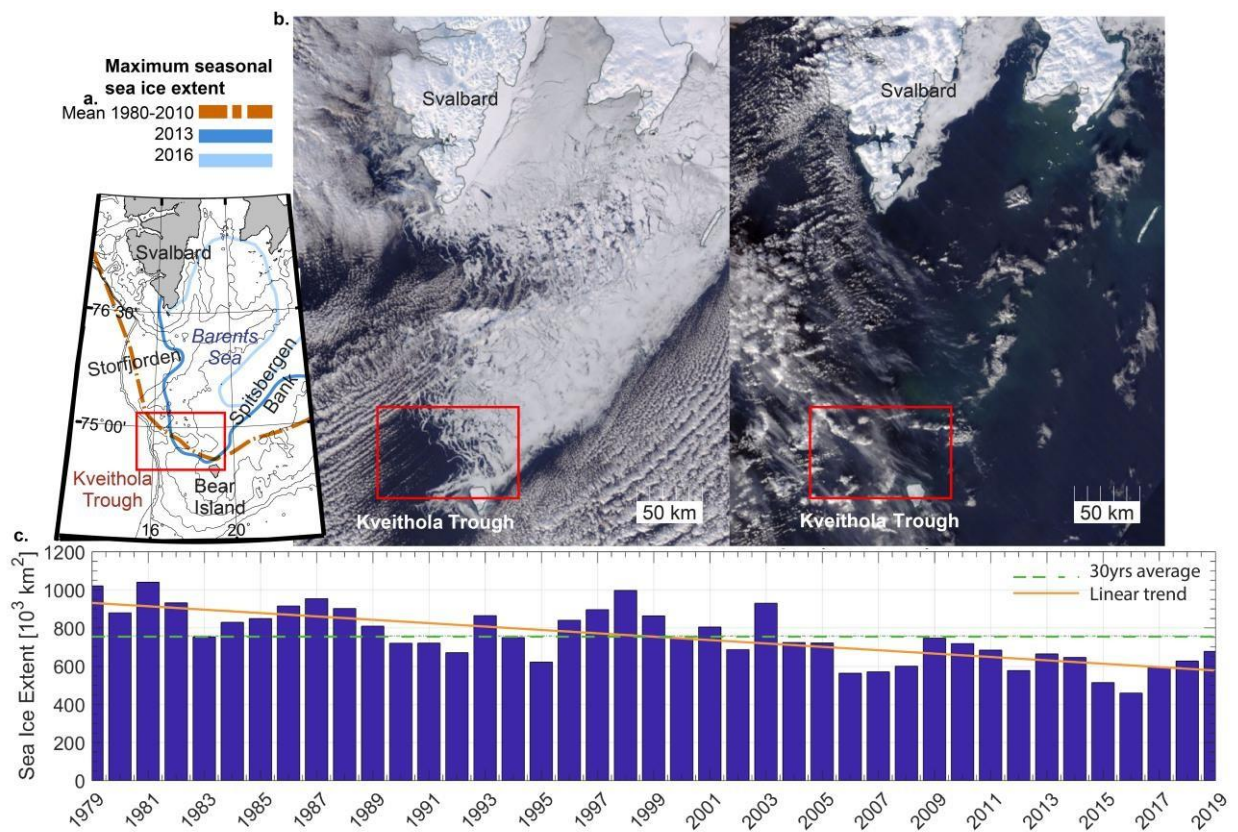


Fig. 5. (a) Map of the Barents Sea showing the average maximum seasonal sea ice extent during 1980-2010 (orange dashed line), in 2013 (dark-blue line), and in 2016 (light-blue line) (NSIDC,

1
2
3
4 <https://nsidc.org/>). (b) Satellite images (Terra/Modis, true-colour corrected reflectance) from 8 March
5
6
7 2013 (on the left) and 12 March 2016 (on the right) showing the maximum seasonal sea ice extent in the
8
9 north-western Barents Sea (the Svalbard Archipelago and the Storfjorden are visible in the northern part
10
11 of the images). (c) Time series of the mean monthly sea-ice extent in April in the Barents Sea, the month
12
13 that normally has the largest sea-ice coverage in the area (Norwegian Polar Institute, www.mosj.no) for
14
15 the period 1979 - 2019. The 30 years-average value (green dashed line) and the linear trend (yellow line)
16
17 throughout the period are also indicated.
18
19
20
21

22 4.3 Grain size and sedimentation rate (SR)

23
24
25
26 The general grain size for the upper 10 cm of the multicore from station 02 is silt-fine sand (63-150 μm),
27
28 coarse silt (31-63 μm) in station 21, and medium to coarse silt (8-15 μm -6 phi) in station 07 (Tab. 1).
29
30
31

32 Activity-depth profiles of excess ^{210}Pb show a quasi-exponential downcore decline, with only small
33
34 fluctuations (supplementary material SF. 1).
35
36
37

38 Station 02, located in the Trough mouth, is characterised by the lowest average SR (on avg. 0.08 cm/yr).
39
40 Stations 21 and 07 have higher sedimentation rates 0.13 and 0.22 cm/yr, respectively. ^{137}Cs activities are
41
42 very low, often below the detection limit. However, at station 07, the Chernobyl peak of 1986 is
43
44 recognizable, supporting SR values based on the ^{210}Pb profile. The obtained values of SR are comparable
45
46 with those previously reported for the Barents Sea (e.g., Zaborska et al., 2008). Based on calculated SRs,
47
48
49 the analysed sedimentary intervals span from 115 years (station 02) to 43 (station 07) (supplementary
50
51 material ST. 1).
52
53
54
55
56
57
58
59
60
61
62
63
64
65

4.4 General faunal distribution and diversity indexes

The analysis of the living benthic foraminifera (size fraction $\geq 150 \mu\text{m}$) have identified 23 species, where 19 are calcareous and 4 species agglutinated. In general, the living foraminiferal assemblages are mainly composed by *ca.* 70-80% of calcareous taxa and 18-26% of agglutinated taxa (Fig. 6; Tab. 2). The highest number of living foraminiferal individuals is found at station 07 with 149 individuals. Yet, station 02 show a more diverse fauna with 15 species. For all the stations, the highest concentration of living foraminifera is found in the first 2- 3 cm bsf. The maximum concentration is registered at station 07 with 5 spec./g at 2 cm bsf. At this station, the living foraminifera are also found down to the maximum depth of 9 cm bsf (Fig. 7). Generally, the dominance value (D) increases to 1 cm down core indicating the predominance of a few or only one species. Station 02 show a high diversity of the living assemblage with a total D value of 0.1 (Tab. 2). Shannon (H) values decreases to 0 when depth increases, and only one taxon is present.

In the dead foraminiferal assemblages (fraction $\geq 150 \mu\text{m}$), 68 benthic foraminiferal species (50 calcareous and 18 agglutinated) are identified. The distribution of the dead foraminiferal assemblage in the topmost 10 cm of sediment show a dominance of the calcareous species, which constitutes more than 95% in all the stations. The agglutinated species are present with a maximum of 2% at station 07. The number of taxa (S) ranges between 36 (station 21) and 49 (station 02). The concentration is 160 to 4977 spec./g, of which the major contributor is the calcareous group (see supplementary material ST. 2). For all the stations D values are relatively low (0.1 to 0.2 max.), indicating the equal presence of all the species in the assemblage. These values are in agreement with the high H values indicating many taxa with a few individuals in the assemblage. The calcareous benthic foraminifera are present in the entire record in all the stations, while the agglutinated foraminifera occur sporadically (see supplementary material ST 2 and 3).

1
2
3
4 Tab. 2: Foraminiferal concentrations and diversity data for each core in the size fraction $\geq 150 \mu\text{m}$. Number
5
6
7 of counted specimens (N), number of species (S), number of foraminiferal specimens per gram of
8
9 sediment (spec./g), Dominance (D) and Shannon index (H). The total values are also indicated in bold font.
10
11 See supplementary material ST. 2 and ST. 3 for the separate values for the calcareous and agglutinated
12
13
14 groups.
15
16

Station	Core depth (cm) bsf	Living foraminiferal assemblages					Dead foraminiferal assemblages				
		N	S	spec./g	D	H	N	S	spec./g	D	H
02	0-0.5	25	8	3	0.2	1.9	403	29	3094	0.1	2.3
	0.5-1	15	8	2	0.2	1.9	337	30	3280	0.1	2.5
	1-1.5	2	2	0.2	0.5	0.7	302	28	2262	0.1	2.5
	1.5-2	4	2	0.4	0.5	0.7	342	27	4661	0.1	2.4
	2-3	3	2	0.2	0.6	0.6	313	26	4977	0.1	2.5
	3-4	-	-	-	-	-	420	26	3313	0.1	2.4
	4-5	2	2	0.1	0.5	0.7	315	29	4161	0.1	2.6
	5-6	-	-	-	-	-	286	27	3272	0.1	2.4
	6-7	2	2	0.1	0.5	0.7	368	25	4187	0.1	2.5
	7-8	-	-	-	-	-	310	21	2477	0.1	2.4
8-9	-	-	-	-	-	363	23	1509	0.2	2.2	
9-10	-	-	-	-	-	325	22	2424	0.2	2.1	
	0-10 (total)	52	15	0.3	0.1	2.4	4084	49	3357	0.1	2.5
21	0-0.5	7	3	1	0.6	0.8	302	25	4069	0.1	2.7
	0.5-1	29	6	4	0.4	1.2	373	29	3478	0.1	2.6
	1-1.5	10	3	1	0.7	0.6	351	22	3431	0.1	2.3
	1.5-2	6	3	1	0.4	1.0	585	24	4709	0.1	2.5
	2-3	-	-	-	-	-	339	23	2921	0.1	2.3
	3-4	1	1	0.1	1.0	0.0	418	22	2556	0.1	2.3
	4-5	-	-	-	-	-	386	26	2664	0.1	2.4
	5-6	-	-	-	-	-	425	20	4135	0.1	2.3
	6-7	-	-	-	-	-	524	22	8960	0.1	2.3
7-8	-	-	-	-	-	567	20	6998	0.1	2.4	
	0-8 (total)	53	8	0.5	0.4	1.3	4270	36	4944	0.1	2.4
07	0-0.5	22	9	2	0.2	2.0	377	38	160	0.1	2.9
	0.5-1	11	3	1	0.5	0.9	303	29	184	0.1	2.8
	1-1.5	11	3	1	0.4	0.9	296	26	165	0.1	2.8
	1.5-2	43	5	5	0.5	0.8	376	32	191	0.1	2.8
	2-3	28	4	2	0.4	1.1	318	30	232	0.1	2.6
	3-4	17	3	1	0.7	0.6	340	30	130	0.1	2.7
	4-5	6	3	0.3	0.4	1.0	247	29	302	0.1	2.7
	5-6	5	3	0.3	0.4	1.1	355	29	192	0.1	2.7
	6-7	4	2	0.2	0.6	0.6	322	28	222	0.1	2.8
	7-8	3	1	0.2	1.0	0.0	334	25	187	0.1	2.7
8-9	1	1	0.1	1.0	0.0	321	27	205	0.1	2.6	
9-10	-	-	-	-	-	339	25	318	0.1	2.6	
	0-10 (total)	149	12	0.85	0.3	1.6	3928	48	214	0.1	2.8



Fig. 6. Cumulative abundance (%) for foraminiferal test of different composition in the living and dead assemblage at each station: calcareous (calcareous perforate), miliolids (calcareous imperforate) and agglutinated. Note that the vertical axis starts at 50%.

14
15
16
17
18
19
20
21
22
23
24
25
26
27
28
29
30
31
32
33
34
35
36
37
38
39
40
41
42
43
44
45
46
47
48
49
50
51
52
53
54
55
56
57
58
59
60
61
62
63
64
65

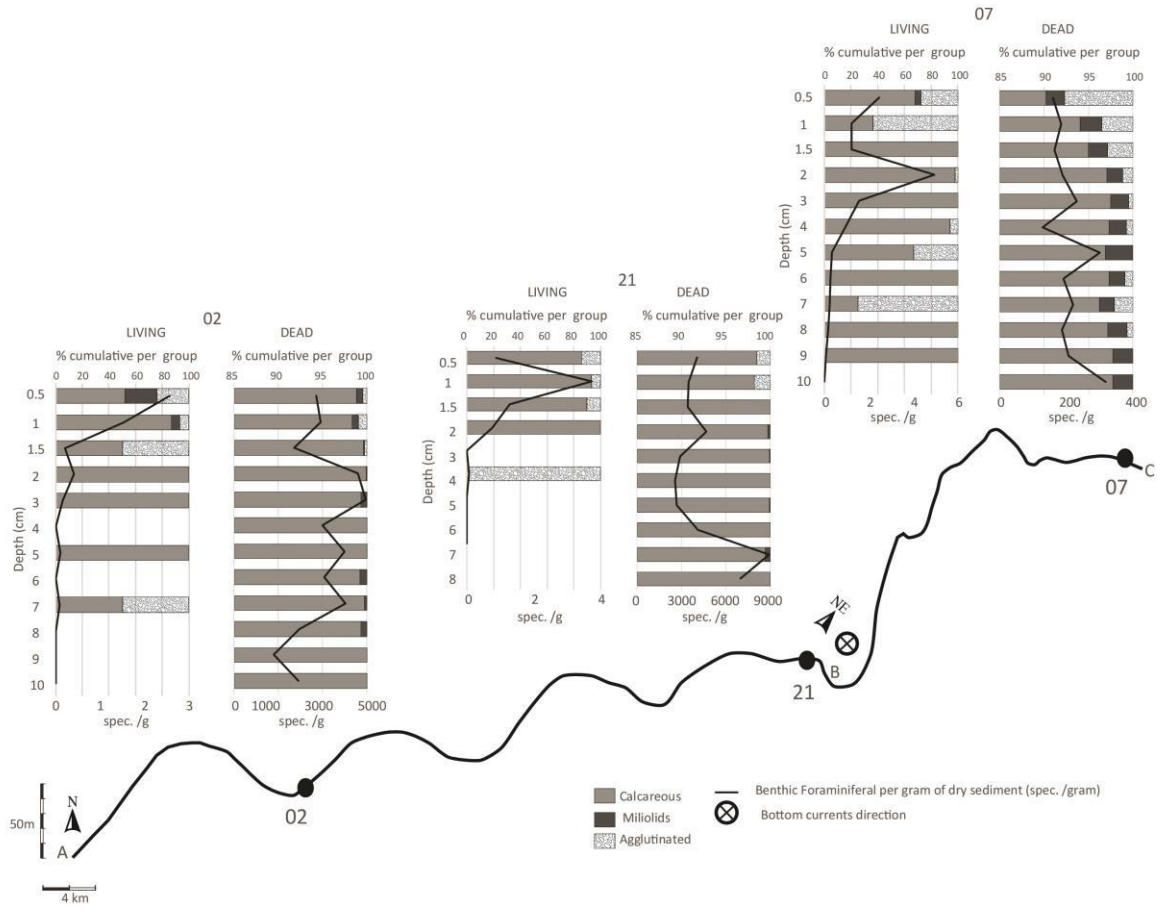


Fig. 7. Downcore living and dead foraminiferal concentrations, and distribution of calcareous (calcareous perforate), miliolids (calcareous imperforate), and agglutinated foraminifera shown along the bathymetric profile of Kveithola Trough. The location of the profile and the way points (A, B, C) are shown in Fig. 1. The black filled circles on the profile are the core locations. **Note that the horizontal axis starts at 85% for the dead foraminifera.**

4.5 Main foraminiferal species

The main calcareous living foraminiferal species are *Cassidulina neoteretis*, *Cibicidoides lobatulus*, *Globobulimina auriculata*, *Islandiella* spp., *Melonis barleeanus*, *Nonionella iridea*, *Nonionellina labradorica*, *Pullenia bulloides* and *Trifarina angulosa* (Fig. 8 and 9; Plate 1). In our study, *T. angulosa* and *P. bulloides* exhibits an epifaunal microhabitat. Few individuals of *P. bulloides* and *C. lobatulus* are also found at 6-7 cm bsf (or deeper), probably transported by the bioturbation process. *C. neoteretis*, *Melonis barleeanus*, *N. labradorica*, *N. iridea* and *Islandiella* spp. show an infaunal habitat. *Globobulimina auriculata* is present in the first upper centimetres of sediment at station 21 and deeper at station 07.

The main dead foraminiferal species include only calcareous species as *Astrononion gallowayi*, *Buccella* spp., *Cassidulina laevigata*, *Cassidulina reniforme*, *C. neoteretis*, *C. lobatulus*, *Elphidium clavatum*, *Globocassidulina subglobosa*, *Islandiella* spp., *M. barleeanus*, *N. labradorica*, *Rotaliida* spp. and *T. angulosa* (Fig. 8 and 9; Plate 1).

The agglutinated foraminifera show high percentages (ca. 20-25%; Fig. 6) in the living foraminiferal assemblages. In all the stations, they are mainly represented by *Reophax* spp. including *Reophax scorpiurus* and *Reophax fusiformis*. In the dead foraminiferal assemblages, the agglutinated species occur with less than 2%, and only in stations 02 and 07. The main agglutinated species group is *Reophax* spp. Only few of the specimens are well preserved, whereas most *Reophax* spp. are partially or totally broken (Fig. 6; Plate 2).

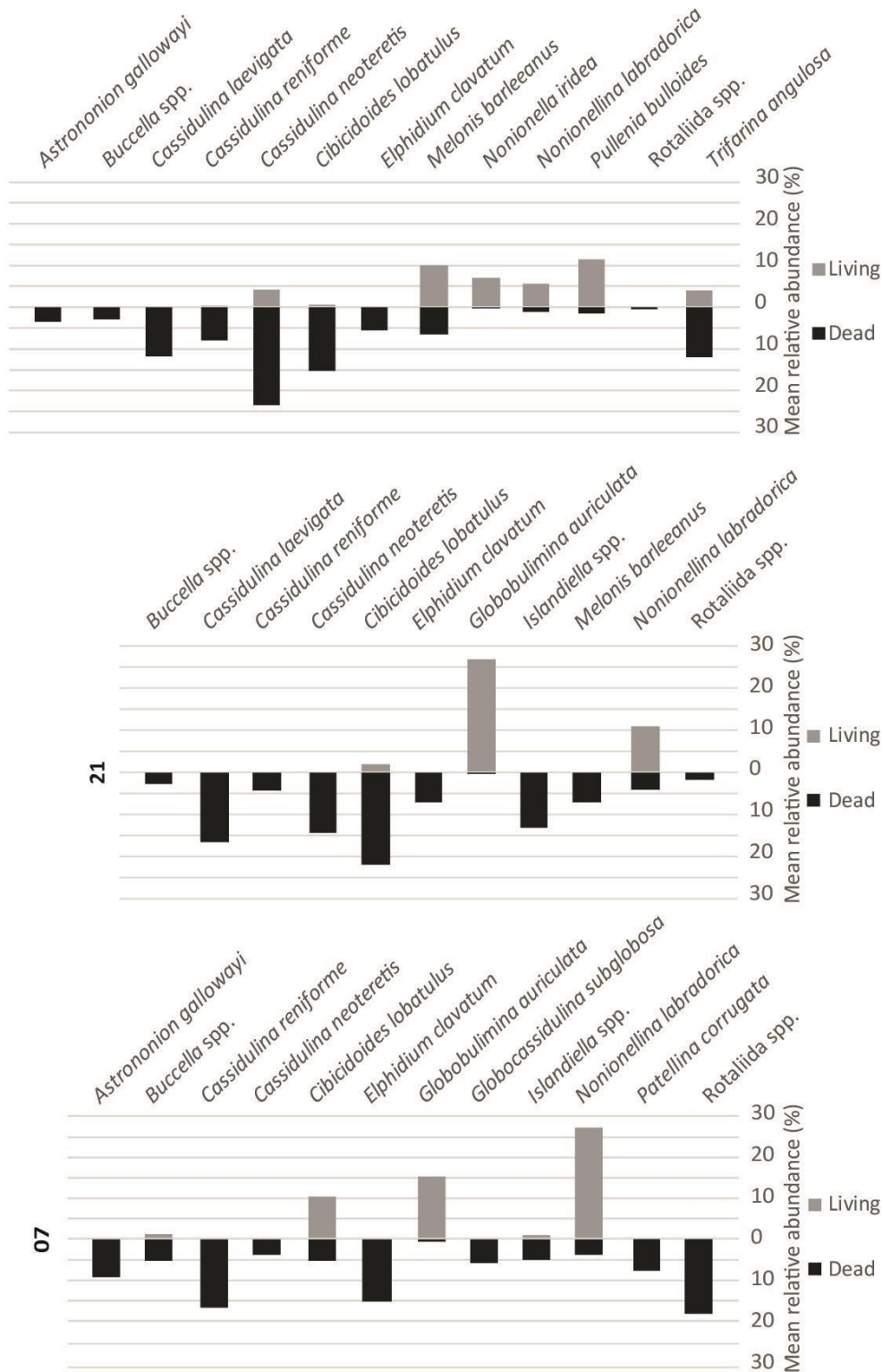


Fig. 8. Mean relative abundance of the main living and dead foraminiferal species, within the upper 0-10 cm of the studied cores.

1
2
3
4
5
6
7
8
9
10
11
12
13
14
15
16
17
18
19
20
21
22
23
24
25
26
27
28
29
30
31
32
33
34
35
36
37
38
39
40
41
42
43
44
45
46
47
48
49
50
51
52
53
54
55
56
57
58
59
60
61
62
63
64
65

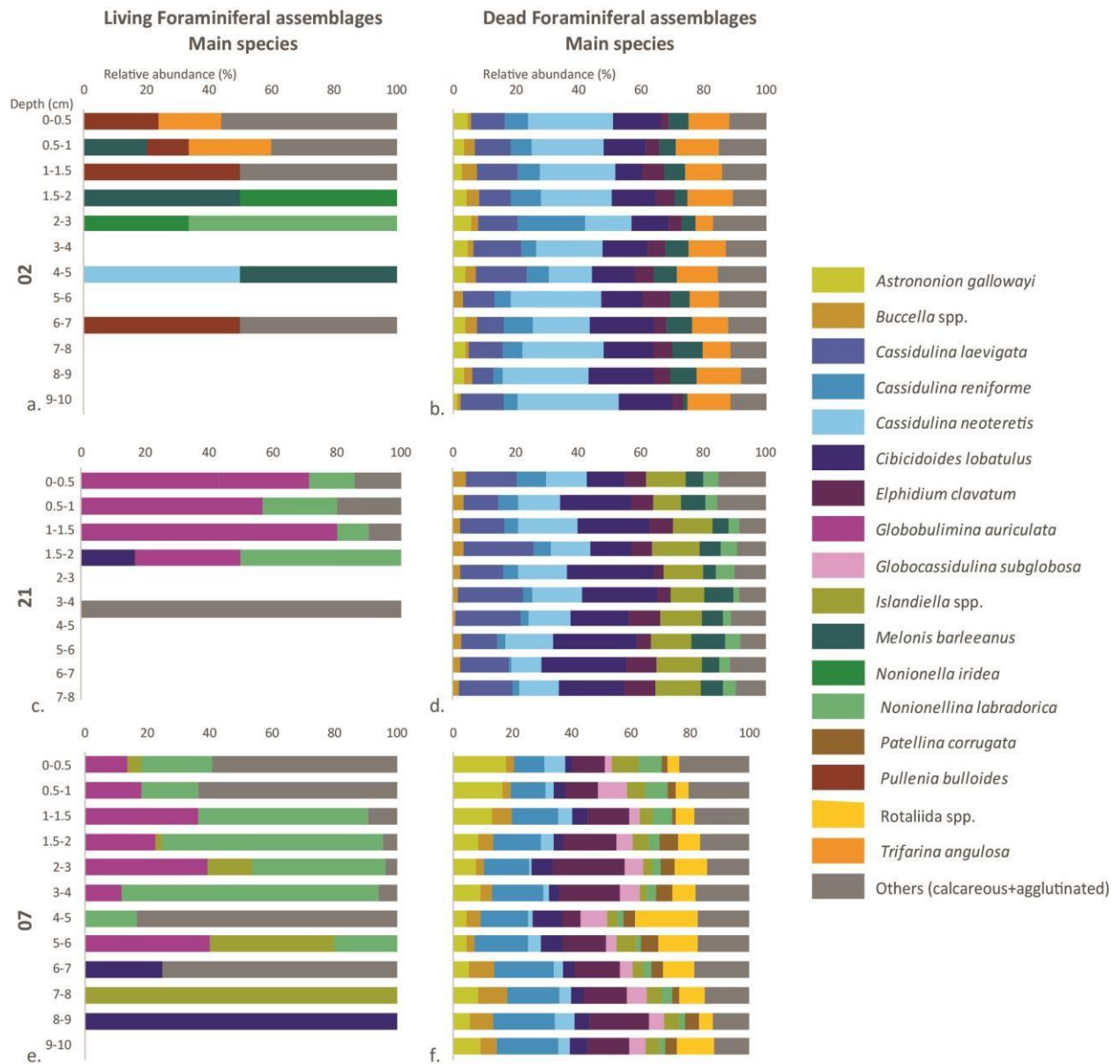


Fig. 9. Down core relative abundance of the main living and dead foraminiferal species.

1
2
3
4 The I/(I+d) ratios have been calculated for the main living and dead foraminiferal species (Tab. 3). The
5
6
7 species *N. iridea* and *N. labradorica* are main contributors to the living foraminiferal assemblage at the
8
9 three stations, whereas, for the dead foraminiferal assemblage, the abundance of the species vary
10
11 throughout the trough. At station 02, the living species *M. barleeanus*, *N. iridea*, *N. labradorica* and
12
13 *P. bulloides* are the most abundant species, whereas *C. reniforme*, *C. neoteretis*, *C. lobatulus* and
14
15 *T. angulosa* are most frequent in the dead assemblage. At station 21 *G. auriculata*, *N. iridea*, *N. labradorica*
16
17 are more abundant in the living assemblage than in the dead assemblage. In the dead assemblage at the
18
19 station 21, the most abundant species are *C. lobatulus* and *P. bulloides*. At station 07, the most frequent
20
21 living species are *C. lobatulus*, *G. auriculata*, *N. iridea* and *N. labradorica*, while it changes in the dead
22
23 assemblage to *Buccella* spp. and *M. barleeanus*.
24
25
26
27
28
29
30
31
32
33
34
35
36
37
38
39
40
41
42
43
44
45
46
47
48
49
50
51
52
53
54
55
56
57
58
59
60
61
62
63
64
65

Tab. 3: Relative abundance of the main foraminiferal species in the living and dead assemblages, and the relative contribution of the main living species (l/(l+d). The black boxes show the higher relative contribution of the living foraminiferal fauna (0.4 to 1.00). The grey boxes show the higher relative contribution of the dead foraminiferal fauna (0.01 to 0.39). Main species that were only present in the dead or living assemblages are also listed. Note *N. iridea* and *P. bulloides* were only main species at the station 02 in the living assemblage; however, their values in other stations are shown.

% Main Species	02			21			07		
	LIVING (l)	DEAD (d)	l/(l+d)	LIVING (l)	DEAD (d)	l/(l+d)	LIVING (l)	DEAD (d)	l/(l+d)
<i>Astrononion gallowayi</i>	0	3.31	0	0	1.95	0	0	9.21	0
<i>Buccella</i> spp.	0	2.76	0	0	2.50	0	1.14	5.24	0.18
<i>Cassidulina laevigata</i>	0	11.59	0	0	16.33	0	0	1.27	0
<i>Cassidulina reniforme</i>	0.33	7.76	0.04	0	4.11	0	0	16.62	0
<i>Cassidulina neoteretis</i>	4.17	23.31	0.15	0	14.04	0	0	3.81	0
<i>Cibicidoides lobatulus</i>	0.56	14.89	0.04	1.85	21.72	0.08	10.42	5.18	0.67
<i>Elphidium clavatum</i>	0	5.30	0	0	6.92	0	0	15.24	0
<i>Globobulimina auriculata</i>	0	0.03	0	27.00	0.20	0.99	15.16	0.67	0.96
<i>Globocassidulina subglobosa</i>	0	0.42	0	0	1.30	0	0	5.73	0
<i>Islandiella</i> spp.	0	0.58	0	0	12.89	0	0.38	4.97	0.07
<i>Melonis barleeanus</i>	10.00	6.32	0.61	0	6.84	0	0	0.43	0
<i>Nonionella iridea</i>	6.94	0.04	0.99	0.74	0	1.00	0.38	0	1.00
<i>Nonionellina labradorica</i>	5.56	0.85	0.87	10.85	4.00	0.73	27.32	3.71	0.88
<i>Patellina corrugata</i>	0	0.18	0	0	0.10	0	0	3.93	0
<i>Pullenia bulloides</i>	11.44	1.32	0.90	0.70	4.02	0.15	0	0.47	0
<i>Rotaliida</i> spp.	0	0.14	0	0	0.84	0	0	9.32	0
<i>Trifarina angulosa</i>	3.89	11.85	0.25	0	0.17	0	0	0.08	0

5. Discussion

5.1 Living foraminiferal assemblages and modern oceanographic conditions.

The distribution of foraminiferal fauna sampled in 2016 along the Kveithola transect reveal a strong variability in the seabed conditions, water column characteristics, and trophic status along the trough and on the shelf.

Station 02, in the outer trough, is strongly dominated by Atlantic water throughout the water column at the moment of the sediment sampling, which probably caused relatively high density and diversity of the living foraminiferal assemblage (Tab. 2). The living foraminiferal assemblage is also dominated by *M. barleeanus*, which thrives within relatively warm Atlantic water (Tab. 4). The vertical distribution of the living foraminiferal fauna is limited to 6- 7 cm bsf (Figs. 7 and 9) and dominated by the detritivore *M. barleeanus*, *P. bulloides* and *T. angulosa*. The living faunal distribution may indicate oligotrophic conditions (Tab. 4), and the bioavailable carbon value (BAC) is low at this station (Tab. 1). This is consistent with a limited supply of nutrition caused by less sea ice in the core site in the winter 2016, hence resulting in reduced seasonal algal blooms (Sakshaug and Slagstad, 1992; Wassmann et al., 1994) and less nutrition to the seabed.

At station 21, in the inner part of the trough, the bottom environment is characterised by different oceanographic conditions than station 02. Station 21 is more influenced by cold and less saline shelf waters. In addition, station 21 is influenced by intermittent seepage activity, where the accumulation of organic matter causes oxygen decrease within the sediment (Tab. 1). Here, the benthic assemblage is dominated by *G. auriculata* related to dysoxic environments and *N. labradorica*, which is typically associated with organic-rich sediments (Corliss, 1991; Koho et al., 2008) (Tab. 4). *N. labradorica* is a deep infaunal species that feeds mainly on the buried organic matter (Corliss, 1991). *Globobulimina* genus

1
2
3
4 usually lives in meso-eutrophic settings, deep in the sediments within or below the oxic-redox interface
5
6
7 (e.g. Licari et al., 2003; Koho et al., 2008). These two taxa may become very abundant if rich sources of
8
9 food are available, acting also as indicators of highly productive conditions (e.g., Jernas et al., 2018). Due
10
11 to the intermittent seepage activity observed in the area (Lucchi et al., 2016; Bazzaro et al., 2020) and the
12
13 presence of dysoxic indicators, we suppose the existence of a strong oxygen gradient at the water-
14
15 sediment interface. *Nonionellina* and *Globobulimina* taxa are not considered endemic to seeps,
16
17 nevertheless, they belong to genera that can respire nitrate instead of oxygen in environments where
18
19 sulphurs are commonly present (Rathburn et al., 2003; Levin, 2005). This stressed environment could also
20
21 cause the low faunal density and diversity (Tab. 2) and the vertical distribution of the living foraminiferal
22
23 fauna, which is limited to the first 4 cm (Figs. 2, 3 and 9).
24
25

26
27
28
29 Station 07, in the north-eastern part of the study area, is mainly dominated by cold (<5°C) and less saline
30
31 (<35) shelf waters. The core site is also influenced by sea ice in the winter 2016 (Fig. 5) and when seasonal
32
33 sea ice melts during the spring primary productivity is enhanced (Sakshaug and Slagstad, 1992). These
34
35 environmental conditions can explain the accumulation of organic matter driving the proliferation of
36
37 abundant foraminiferal fauna, dominated by *Nonionella* spp. and *G. auricula*. The vertical distribution of
38
39 benthic fauna down to 9 cm bsf (Tab. 1) may be related with the more oxygenated bottom waters, which
40
41 favour the oxygen penetration into the sediments. Caridi et al. (2019) reported for the same station, a
42
43 high macrofaunal bioturbation activity that can favour both the oxygen penetration and the mobility of
44
45
46
47
48 **the foraminifera in the first centimetres of the sediment.**
49
50
51
52
53
54
55
56
57
58
59
60
61
62
63
64
65

5.2 Preservation and taphonomic processes

The living foraminiferal assemblages register a specific moment of environmental conditions, which improves our understanding of the environmental ranges of the observed species. The dead foraminiferal assemblages correspond to an average of the environmental conditions over time interval, which may record several years of deposition in a specific area. This improves our understanding of the dynamics of foraminiferal assemblages over the time. Therefore, in our study, the living foraminiferal assemblages gave an observation of the environmental conditions during the summer (June) 2016, while the dead foraminiferal assemblages showed the changes occurring over a larger temporal interval, giving an average of environmental conditions throughout several years (including all seasons).

The living foraminiferal assemblages can appear different from the dead foraminiferal assemblages leading to a correlation of different environmental conditions (Murray and Alve, 1999). The taphonomic processes, e.g. dissolution and desegregation, damage the foraminiferal test contributing to differences between living and dead foraminiferal assemblages.

In our stations, the main difference between living and dead assemblages is the preservation of the agglutinated species (Figs. 6 and 7). The occurrence of agglutinated foraminifera is partially or totally subordinated to that of calcareous species in both the living and dead assemblages due to major preservational problems (Fig. 6). Agglutinated foraminifera have a poor preservation potential due to the mechanical disaggregation, test compaction and degradation of the organic cement that binds together the agglutinated grains (Schröder, 1988; Murray, 2006). Furthermore, also the calcareous or iron compounds of agglutinates cement may dissolve or oxidize (De Stigter et al., 1999; Duros et al., 2014; Dessandier et al., 2018). Our results show an increase of broken agglutinated test below the first centimetres of sediments (Fig. 6), and the disappearance of the agglutinated taxa deeper in the sediment

1
2
3
4 (Fig. 7), both in oxygenated and dysoxic environments. Some studies (e.g., Schröder, 1988; De Stigter et
5
6 al., 1999) have already pointed to this taphonomic process in different oceanographic contexts, estimated
7
8 the loss of the dead agglutinated taxa of about 20% compared to the living species.
9

10
11
12
13 The calcareous foraminiferal tests suffer different mechanisms that can lead to their partial or total
14
15 destruction (Murray, 2006). The dissolution affects especially the delicate and/or aragonitic calcareous
16
17 tests. Species with delicate tests, such as *G. auriculata* (Ellis and Messina, 1940-1978), is very frequent in
18
19 the living foraminiferal assemblages (Tab. 3; Fig. 8 and 9), yet its frequency is reduced in the dead
20
21 foraminiferal assemblages, and many broken specimens have been observed (Plate 2). In this study, we
22
23 have also frequently observed specimens of *Nonionellina labradorica* and *Nonionella iridea* having a
24
25 broken ultimate chamber (Tab. 3; Figs. 8 and 9, Plate 2). The calcareous species also showed marks of
26
27 predation like different boring patterns, holes and cavities that may be produced by phototrophic
28
29 (cyanobacteria, chlorophyta) and heterotrophic (fungi) organisms (Cherchi et al., 2012). This predation
30
31 weakens the test facilitating or producing the mechanical disaggregation of the test (Plate 2). In all these
32
33 cases, the species are classified as detailed as possible especially in the cases when the fragment included
34
35 the proloculus and/or the aperture zone, for which a correct classification could be made.
36
37
38
39
40

41
42 Post-mortem bioturbation and reworking of the sediments may also have caused fragmentation,
43
44 corrosion and disintegration of the foraminiferal tests (Schröder, 1988; De Stigter et al., 1999; Loubere et
45
46 al., 2011; Duros et al., 2014; Dessandier et al., 2018). These processes intensified with the increase of the
47
48 amount of macrofauna, as described in Caridi et al. (2019). Bioturbation would facilitate the decrease or
49
50 even the disappearance of some taxa from the dead foraminiferal record, especially for those specimens
51
52 having delicate tests that are weaker or not well cemented (Tab. 3; Figs. 6 and 8; Plate 2).
53
54

55
56
57 **In general, most calcareous specimens are found in good condition; hence, we are confident of suitability**
58
59 **and quality of the foraminiferal record for paleoenvironmental reconstructions. The comparisons**
60
61

1
2
3
4 between living and dead foraminiferal concentration (spec./g, Tab. 3) suggest a good preservation of most
5
6
7 of the species. The dead foraminiferal assemblages include all the living foraminiferal species although
8
9 occurring with different percentages. When comparing it should be taken into account that living
10
11 foraminiferal assemblages represent specific environmental conditions while the dead foraminiferal
12
13 assemblages represent a larger time interval and an average of yearly environmental characteristics.
14
15 However, the current good agreement between assemblages indicate that the dead foraminiferal
16
17 assemblages are robust paleoenvironmental indicators.
18
19

20 21 22 5.3 Paleoenvironmental variations during the last decades 23

24
25
26 The sedimentary records used for this study cover the last *ca.* 50-100 years (supplementary material
27
28 ST. 1). The composition of the benthic foraminiferal assemblages in all three paleorecords is relatively
29
30 stable, suggesting relatively stable environmental conditions during the investigated time interval.
31
32

33
34 The paleorecord from the outer trough, station 02 covers the last 115 years and is characterised by sandy
35
36 sediments (Tab. 1). This suggests relatively strong bottom currents, which is also reflected by *C. lobatulus*
37
38 that is often associated with higher dynamic environments (Fig. 4; Tab. 4). These high-energy conditions
39
40 provided a constant supply of organic matter and oxygen, which probably increased the diversity of the
41
42 assemblage (Tab. 2). Furthermore, the presence of *C. reniforme*, and *C. neoteretis*, with the warm-water
43
44 indicator *C. laevigata* suggest a relatively strong influence by warm AW (Fig. 9). The foraminiferal record
45
46 also show some influence of colder waters and sea ice at the station 02 during the last decades. At
47
48
49
50
51 2- 3 cm bsf (*ca.* 1986), both the frequency of cold-water species *C. reniforme* (Fig. 9) and the sea ice data
52
53 increase (Fig. 5).
54

55
56
57 During the last *ca.* 64 years, the inner trough station (21), has recorded relatively stable environmental
58
59 conditions. The presence of *Islandiella* spp. and *N. labradorica* indicate relatively higher trophic level.
60
61

1
2
3
4 Mesotrophic to eutrophic conditions could be related to the position of the core site close to the sea ice
5
6
7 margin where high biological productivity can facilitate an accumulation of organic matter to the bottom
8
9 (Tab. 2 and 4; Fig. 9). The increased abundance of *Islandiella* spp., compared to station 02, indicates an
10
11 increase of nutrients, probably related to a stronger influence of the marginal sea ice zone (Fig. 5). The
12
13 foraminiferal assemblage also contains *C. laevigata*, *C. neoteretis* and *C. reniforme*, similar to station 02;
14
15 reflecting comparable water masses conditions, with influence of both the relatively warm (AW) and cold
16
17 water masses.
18
19

20
21
22 The record from the shelf area (station 07), which covers the last *ca.* 43 years, is characterised by fresher
23
24 and colder waters, in accordance with its northernmost position, and therefore, the greater influence of
25
26 the Arctic water origin and longer periods of sea ice cover. The colder conditions are shown by the
27
28 predominance of cold-water species *E. clavatum* and *C. reniforme* (Tab. 4). The decrease of species
29
30 indicative of warmer conditions, *Buccella* spp., *Islandiella* spp., *N. labradorica* and *Melonis barleeanus*,
31
32 show less influence of warm AW and the reduction in the quantity or quality of nutrients availability
33
34 compared to the other stations (Fig. 8; Tab. 4).
35
36

37
38
39
40 Previous studies have shown how dead benthic foraminiferal assemblages have changed within the last
41
42 two centuries in the SW and the central Barents Sea, reflecting a warming trend of the Atlantic water
43
44 (Wilson et al., 2011; Dijkstra et al., 2017a). However, these progressively warming conditions are not
45
46 observed in our record from Kveithola Trough possibly due to the extent of the current records (maximum
47
48 *ca.* 100 years), comprising the already advancing warm period. Saher et al. (2012) observe a change to a
49
50 dominance of warm water species between 1965-1992 and 2005-2005, which is probably related to the
51
52 changed position of the ice edge in the central Barents Sea during this time interval. We also speculate
53
54 the Kveithola Trough may have morphological features making it a more protected system as indicated
55
56 by the oceanographic data collected during the cruise.
57
58
59
60
61
62
63
64
65

Tab. 4. Ecological characteristics of the main living and dead species.

MAIN SPECIES	ENVIRONMENTAL CONDITIONS	REFERENCES
<i>Astrononion gallowayi</i>	Temperature tolerant, epifaunal	Saher et al., 2009; Saher et al., 2012.
<i>Buccella</i> spp.	Cold water, infaunal, often related to oceanic fronts/sea ice edges	Steinsund, 1994; Hald and Korsun, 1997; Saher et al., 2009; Saher et al., 2012.
<i>Cassidulina laevigata</i>	Warm water, infaunal	Sejrurp et al., 2004; Saher et al., 2009; Steinsund, 1994; Dijkstra et al., 2017b.
<i>Cassidulina reniforme</i>	Cold water, infaunal	Hald and Korsun, 1997; Korsun and Hald, 1998; Murray, 2006; Saher et al., 2009; Saher et al., 2012; Dijkstra et al., 2017b.
<i>Cassidulina neoteretis</i>	Cold water, infaunal, associated with cooled Atlantic Water in the Barents Sea, prefers fresh phytodetritus	Saher et al., 2009; Seidenkrantz, 1995; Dijkstra et al., 2017b.
<i>Cibicidoides lobatulus</i>	Temperature tolerant, epifaunal, tolerates high energy environments	Steisund, 1994; Hald and Steisund, 1996; Wollenburg and Mackensen, 1998; Murray, 2006; Saher et al., 2009; Saher et al., 2012.
<i>Elphidium clavatum</i>	Cold water, infaunal, tolerates less than marine salinity	Steinsund, 1994; Sejrurp et al., 2004; Murray, 2006; Saher et al., 2009; Saher et al., 2012; Dijkstra et al., 2017b.
<i>Globbulimina auriculata</i>	Temperature tolerant, infaunal, facultative anaerobe, tolerates dysoxia, detritivore	Gooday et al., 2001; Murray, 2006; Murray and Alve, 2016.
<i>Globocassidulina subglobosa</i>	Cold water, infaunal, low organic content, infaunal, detritivore	Murray, 2006.
<i>Islandiella</i> spp.	Cold water, infaunal, free, detritivore, high availability of nutrition	Steinsund, 1994; Murray, 2006; Saher et al., 2009; Saher et al., 2012; Dijkstra et al., 2017b.
<i>Melonis barleeanus</i>	Relatively warm water, infaunal, tolerates dysoxia, detrivore, related to degraded organic matter	Steinsund, 1994; Murray, 2006; Saher et al., 2009; Saher et al., 2012; Dijkstra et al., 2017b.
<i>Nonionella iridea</i>	Cold water, infaunal, phytodetritus species, infaunal	Murray, 2006.
<i>Nonionellina labradorica</i>	Cold water, infaunal, associated with high availability of nutrition	Sejrurp et al., 2004; Murray, 2006; Saher et al., 2009; Saher et al., 2012.
<i>Patellina corrugata</i>	Temperature tolerant, epifaunal, associated with high availability of nutrition	Murray, 2006
<i>Pullenia bulloides</i>	Temperature tolerant, infaunal, detrivore	Murray, 2006; Saher et al., 2009.
<i>Trifarina angulosa</i>	Temperature tolerant, epifaunal, tolerates high energy environments	Steinsund, 1994; Murray, 2006; Saher et al., 2009.

6. Conclusions

Geological and oceanographic data collected during the Eurofleets 2- BURSTER cruise in June 2016 reveal a highly dynamic marine environment in the Kveithola Trough.

The CTG-labelled living foraminiferal from the outer station (02) influenced by AW, show that the living foraminiferal assemblages are dominated by the warm water species *M. barleeanus* and the tolerant temperature species, *P. bulloides*. In the inner station 21, the living foraminiferal assemblages is dominated by the high food supply indicator *N. labradorica*, and by the dysoxia species, *G. auriculata* related to the presence of methane seepage. The shelf station (07) is dominated are by *G. auriculata*, *N. labradorica* and the high-dynamic environmental indicator, *C. lobatulus*. The dominance of warmer water species in the outer shelf and the presence of eutrophic species in the inner part of the trough reflect the oceanographic conditions during the sampling period and the high availability of organic matter to the seafloor.

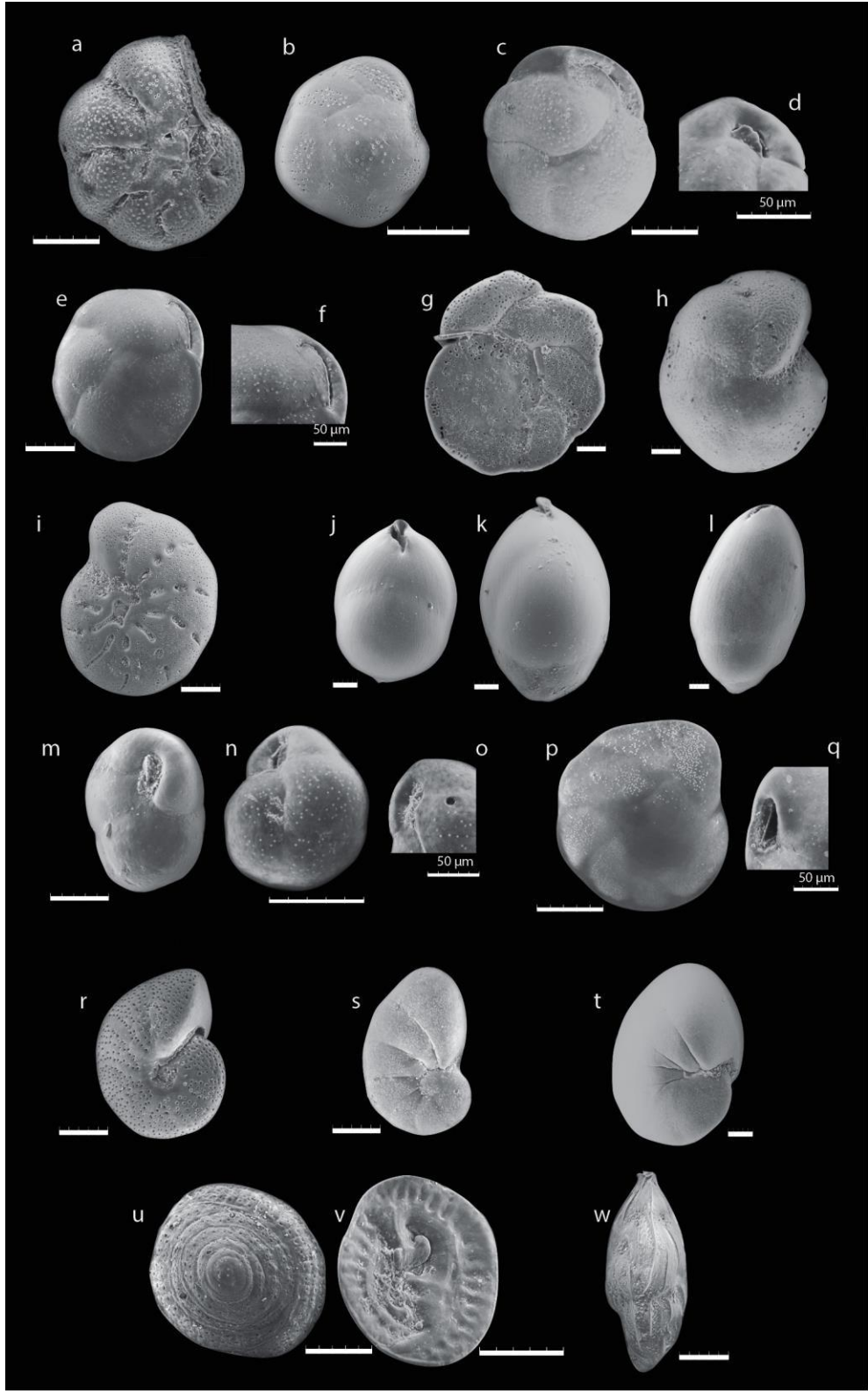
The taphonomical processes affect the preservation of the foraminiferal test, especially the agglutinated foraminifera, increasing the possibility of bias in the paleoenvironmental interpretation when using these taxa. We have found the preservation of most of the calcareous species is good, and they may contribute to robust paleoenvironmental records.

The dead foraminiferal assemblages show no significant changes during the last *ca.* 100 years. At station 02, the dead foraminiferal assemblages show the influence of relatively warm AW by *C. laevigata* and *C. neoteretis* and relatively strong hydrodynamic conditions by *C. lobatulus*. The paleoenvironmental record at station 21 shows similar conditions to the outer part of the trough. Yet the increased abundances of *Islandiella* spp. and *N. labradorica* indicate a higher trophic level probably reflecting an increased influence of seasonal sea ice and increased nutrient influx. The dominant species at station 07 are the

1
2
3
4 cold-water indicators *C. reniforme* and *E. clavatum*, mirroring to the northern position of this station with
5
6 a larger influence of colder water and sea ice.

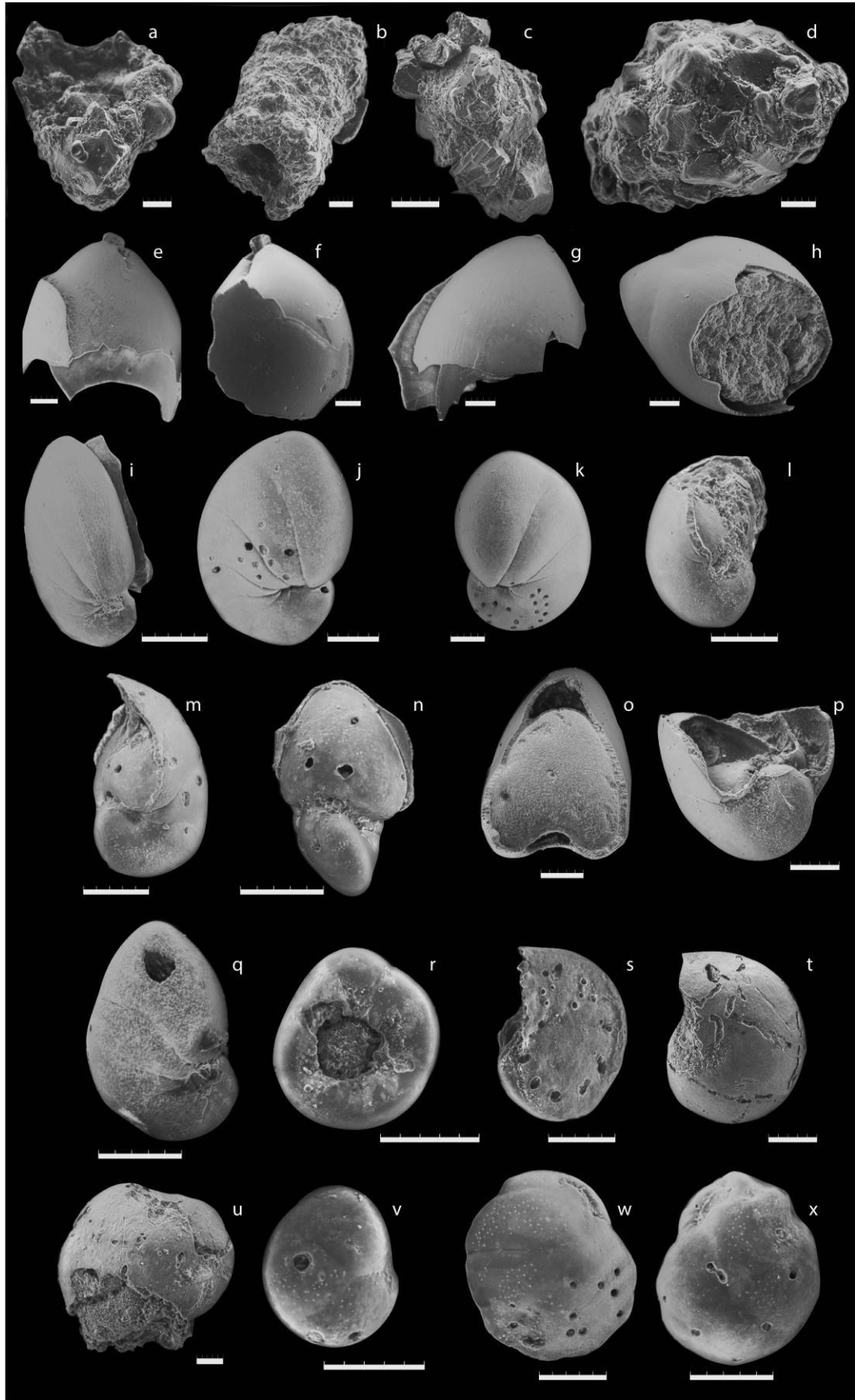
7
8
9
10 The dead foraminiferal assemblages in Kveithola Trough show no significant changes during the last
11
12
13 *ca.* 100 years. In contrast to other studies from other areas of the Barents Sea that indicate a larger and
14
15 progressively increasing influence of the Atlantic water either within the last 200 years (Wilson et al.,
16
17 2011; Dijkstra et al., 2013) or with the last *ca.* 30 years (Saher et al., 2012). This may be due to the current
18
19 study is shorter than the others are and it does not record pre-impacted conditions or the time interval
20
21 being recorded yet. We also speculate that the local morphology of the Kveithola Trough may protect the
22
23 environmental system from external influences responsible for the changes recorded in other parts of the
24
25 Barents Sea.
26
27
28
29
30
31
32
33
34
35
36
37
38
39
40
41
42
43
44
45
46
47
48
49
50
51
52
53
54
55
56
57
58
59
60
61
62
63
64
65

1
2
3
4
5
6
7
8
9
10
11
12
13
14
15
16
17
18
19
20
21
22
23
24
25
26
27
28
29
30
31
32
33
34
35
36
37
38
39
40
41
42
43
44
45
46
47
48
49
50
51
52
53
54
55
56
57
58
59
60
61
62
63
64
65



1
2
3
4 Plate 1: Some of the main calcareous dead foraminiferal species: (a) *Astrononion gallowayi*;
5
6
7 (b) *Buccella* spp.; (c) *Cassidulina reniforme*, (d) *C. reniforme* zoom of the aperture; (e) *Cassidulina*
8
9 *neoteretis*, (f) *C. neoteretis* zoom of the aperture; (g-h) *Cibicidoides lobatulus*; (i) *Elphidium clavatum*;
10
11 (j- k- l) *Globobulimina auriculata*; (m-n) *Globocassidulina subglobosa*; (o) *G. subglobosa* zoom of the
12
13 aperture; (p-q) *Islandiella* spp.; (r) *Melonis barleeanus*; (s) *Nonionella iridea*; (t) *Nonionellina labradorica*;
14
15 (u) *Patellina corrugata*; and (w) *Trifarina angulosa*. Scale-bar 100 μ m, except for the different measure
16
17 indicated above the scale-bar.
18
19
20
21
22
23
24
25
26
27
28
29
30
31
32
33
34
35
36
37
38
39
40
41
42
43
44
45
46
47
48
49
50
51
52
53
54
55
56
57
58
59
60
61
62
63
64
65

1
2
3
4
5
6
7
8
9
10
11
12
13
14
15
16
17
18
19
20
21
22
23
24
25
26
27
28
29
30
31
32
33
34
35
36
37
38
39
40
41
42
43
44
45
46
47
48
49
50
51
52
53
54
55
56
57
58
59
60
61
62
63
64
65



1
2
3
4 Plate 2: Dead foraminiferal species with taphonomic processes evidences: (a-d) Fragments of agglutinated
5
6
7 foraminifera; (e-h) Fragments of *G. auriculata*; (i-q) *N. iridea* and *N. labradorica*: (i) broken test, (j-k) holes
8
9 (marks predation?), (l-m-n) last chamber broken: (l) partially filled with sediment and (m-n) with holes
10
11 (predation or post mortem activity?), (o) last chamber separate of the rest of the test, (p) total breakage
12
13 of the last chambers, (q) last chamber broken (mechanically?); (r) Rotaliida indet. ventral broken;
14
15 (s- t) *C. lobatulus*: (marks predation?): (s) holes, (t) cavities; (u) *Cassidulina* spp. with marks, broken and
16
17 partially filled; (v) *C. reniforme* holes (marks predation?); and (w-x) *C. neoteretis* holes (marks predation?).
18
19
20
21 Scale-bar 100 μ m.
22
23
24
25
26
27
28
29
30
31
32
33
34
35
36
37
38
39
40
41
42
43
44
45
46
47
48
49
50
51
52
53
54
55
56
57
58
59
60
61
62
63
64
65

Acknowledgments

We would like to firstly acknowledge Eurofleets2 for the great support by funding the data acquisition of the project BURSTER (Bottom currents in a stagnant environment), on-board of the R/V Polarstern (expedition PS99-1). We also thank the Captain, crew and scientific party of exp. PS99-1 and Thomas Soltwedel for the important advice during the cruise preparation and the expedition. Thanks to Massimo Tagliaferro for the basics to the use of SEM during the cruise. Data analyses were funded by the PNRA project AXED (Anoxic environments in Arctic sediment drifts) through the University of Pisa (Italy). The University of Costa Rica is acknowledged for the PhD scholarship to Viviana Maria Gamboa Sojo. The acquired data from the vmADCP were processed after the cruise by Laura Ursella (OGS). Thanks to Karen Gariboldi and Diana Segura Sojo for their comments in the final stages of the writing process.

Author contributions

R.G.L. and **C.M.** conceived and designed the research. **R.G.L.** PI of BURSTER project. **C.M.** PI of AXED project and conceptualization. **V.M.G.S., F.C., A.S., R.G.L., M.B., V.K., A.T.D., P.P., C.M.** acquired data at sea during the BURSTER cruise. **V.M.G.S.** processed and analysed the dead foraminiferal assemblages and living data $\geq 150 \mu\text{m}$. **V.M., C.M.** and **K.H.** analysed the dead foraminiferal assemblages data. **F.C.** and **A.S.** processed and analysed the living foraminiferal assemblages. **R.G.L.** processed sedimentological data. **M.B., V.K.** processed and analysed oceanographic data. **A.T.D.** processed ^{210}Pb and ^{137}Cs radionuclide measurements. **L.L.** and **A.T.D.** calculated ^{210}Pb -based sedimentation rates. **P.P.** carried out grain size analysis. **V.M.G.S.** wrote the most of the manuscript with contributions from: **C.M.** and **K.H.** dead foraminiferal assemblages, preservation and taphonomic processes; **F.C.** and **A. S.** Living foraminiferal assemblages and modern situation; **R.G.L.** grain size and sedimentological analyses; **M.B.** and **V.K.** oceanographic data and water masses properties; **L.L.** and **A.T.D.** age model and sedimentation rate. All authors discussed the results, the conclusions and reviewed the manuscript.

1
2
3
4 References
5
6
7

8 Aagaard, K., 1989. A synthesis of the Arctic Ocean circulation. *Le Conseil. Rapp. P. V. Reun. Cons. Int.*
9
10 *Explor. Mer.* 188, 11 – 22.
11

12
13
14 Aagaard, K., Coachman, L. K., Carmack, E., 1981. On the halocline of the Arctic Ocean. *Deep Sea Research.*
15
16 *Part A* 286, 529-545.
17

18
19
20 Aagaard, K., Swift, J. H., Carmack, E. C., 1985. Thermohaline circulation in the Arctic Mediterranean seas.
21
22 *Journal of Geophysical Research. Oceans* 90C3, 4833-4846.
23

24
25 Aagaard, K., Darnall, C., Greisman, P., 1973. Year-long current measurements in the Greenland-
26
27 Spitsbergen passage. *Deep Sea Research.* 20 (8), 743-746.
28

29
30
31 Bazzaro, M., Ogrinc, N., Relitti, F., Lucchi, R.G., Giani, M., Adami, G., Pavoni, E., De Vittor, C., 2020.
32
33
34 Geochemical signatures of intense episodic anaerobic oxidation of methane in near-surface sediments of
35
36 a recently discovered cold seep (Kveithola trough, NW Barents Sea). *Marine Geology*, 425, 106189.
37

38
39 Bjarnadóttir, L. R., Rüther, D. C., Winsborrow, M. C., Andreassen, K., 2013. Grounding-line dynamics during
40
41 the last deglaciation of Kveithola, W Barents Sea, as revealed by seabed geomorphology and shallow
42
43 seismic stratigraphy. *Boreas*, 42(1), 84-107.
44

45
46
47
48 Bernhard, J. M., Ostermann, D. R., Williams, D. S., Blanks, J. K., 2006. Comparison of two methods to
49
50 identify live benthic foraminifera: A test between Rose Bengal and CellTracker Green with implications for
51
52 stable isotope paleoreconstructions. *Paleoceanography* 214.
53
54
55
56
57
58
59
60
61
62
63
64
65

1
2
3
4 Caridi, F., Sabbatini, A., Morigi, C., Dell'Anno, A., Negri, A., Lucchi, R.G., 2019. Patterns and environmental
5
6
7 drivers of diversity and community composition of macrofauna in the Kveithola Trough NW Barents Sea.
8
9 Journal of Sea Research 153, 101780.
10
11
12 Carpenter, J.H., 1965. The Chesapeake Bay Institute technique for the Winkler dissolved oxygen method.
13
14
15 Limnology and Oceanography 101, 141-143.
16
17
18 Cherchi, A., Buosi, C., Zuddas, P., De Giudici, G.B., 2012. Bioerosion by microbial euendoliths in benthic
19
20
21 foraminifera from heavy metal-polluted coastal environments of Portovesme south-western Sardinia,
22
23 Italy. Biogeosciences 9, 4607–4620.
24
25
26 Comiso, J.C., Hall, D.K., 2014. Climate trends in the Arctic as observed from space. Wiley Interdisciplinary
27
28
29 Reviews: Climate Change 53, 389-409.
30
31
32 Corliss, B.H., 1991. Morphology and microhabitat preferences of benthic foraminifera from the northwest
33
34
35 Atlantic Ocean. Marine Micropaleontology. 173-4, 195-236.
36
37
38 De Stigter, H.C., Van der Zwaan, G.J., Langone, L., 1999. Differential rates of benthic foraminiferal test
39
40
41 production in surface and subsurface sediment habitats in the southern Adriatic Sea. Palaeogeography,
42
43 Palaeoclimatology, Palaeoecology. 1491-4, 67-88.
44
45
46 Dessandier, P.A., Bonnin, J., Kim, J.H., Racine, C., 2018. Comparison of living and dead benthic foraminifera
47
48
49 on the Portuguese margin: Understanding the taphonomical processes. Marine Micropaleontology. 140,
50
51
52 1-16.
53
54
55 Dijkstra, N., Junttila, J., Carroll, J., Husum, K., Hald, M., Elvebakk, G., Godtlielsen, F., 2013. Baseline benthic
56
57
58 foraminiferal assemblages and habitat conditions in a sub-Arctic region of increasing petroleum
59
60
61 development. Marine environmental research, 92, 178-196.
62
63
64
65

1
2
3
4 Dijkstra, N., Junttila, J., Aagaard-Sørensen, S., 2017a. Environmental baselines and reconstruction of
5
6 Atlantic Water inflow in Bjørnøyrenna, SW Barents Sea, since 1800 CE. *Marine Environmental Research*.
7
8 132, 117-131.
9

10
11
12 Dijkstra, N., Junttila, J., Skirbekk, K., Carroll, J., Husum, K., Hald, M., 2017b. Benthic foraminifera as bio-
13
14 indicators of chemical and physical stressors in Hammerfest harbor Northern Norway. *Marine pollution*
15
16 *bulletin*, 1141, 384-396.
17
18

19
20
21 Dowdeswell, J.A., Fugelli, E.M.G., 2012. The seismic architecture and geometry of grounding-zone wedges
22
23 formed at the marine margins of past ice sheets. *GSA Bulletin* 12411-12, 1750-1761.
24

25
26 Duplessy, J.C., Ivanova, E., Murdmaa, I., Paterne, M., Labeyrie, L., 2001. Holocene paleoceanography of
27
28 the northern Barents Sea and variations of the northward heat transport by the Atlantic Ocean. *Boreas*
29
30 301, 2-16.
31
32

33
34
35 Duros, P., Fontanier, C., De Stigter, H. C., Cesbron, F., Metzger, E., Jorissen, F. J., 2012. Live and dead
36
37 benthic foraminiferal faunas from Whittard Canyon (NE Atlantic): Focus on taphonomic processes and
38
39 paleo-environmental applications. *Marine Micropaleontology*, 94, 25-44.
40

41
42
43 Duros, P., Jorissen, F.J., Cesbron, F., Zaragosi, S., Schmidt, S., Metzger, E., Fontanier, C., 2014. Benthic
44
45 foraminiferal thanatocoenoses from the Cap-Ferret Canyon area NE Atlantic: a complex interplay between
46
47 hydro-sedimentary and biological processes. *Deep Sea Research. Part II* 104, 145-163.
48
49

50
51 Ellis, B.E., Messina, A.R., 1940–1978. *Catalogue of Foraminifera*. Micropaleontology Press, Am. Museum
52
53 of Natural History, New York.
54

55
56
57 Feyling-Hanssen, R.W., Jørgensen, J.A., Knudsen, K.L., Lykke-Andersen, A.L., 1971. Late Quaternary
58
59 Foraminifera from Vendsyssel, Denmark and Sandnes, Norway. *Geological Society of Denmark* 21, 67-317.
60
61

- 1
2
3
4 Fohrmann, H., Backhaus, J.O., Blaume, F., Rumohr, J., 1998. Sediments in bottom-arrested gravity plumes:
5
6
7 Numerical case studies. *Journal of Physical Oceanography*. 2811, 2250-2274.
8
9
10 Friedman, G.M., Sanders, J.E., 1978. *Principles of sedimentology*. Wiley, New York.
11
12
13 Gooday, A. J., Hughes, J. A., Levin, L. A., 2001. The foraminiferan macrofauna from three North Carolina
14
15 (USA) slope sites with contrasting carbon flux: a comparison with the metazoan macrofauna. *Deep Sea*
16
17 *Research Part I: Oceanographic Research Papers*, 48(7), 1709-1739.
18
19
20
21
22 Green, K.E., 1960. Ecology of some Arctic foraminifera. *Micropaleontology* 61, 57-78.
23
24
25 Groot, D.E., Aagaard-Sørensen, S., Husum, K., 2014. Reconstruction of Atlantic water variability during the
26
27 Holocene in the western Barents Sea. *Climate of the Past* 101, 51-62.
28
29
30
31 Hald, M., Korsun, S., 1997. Distribution of modern benthic foraminifera from fjords of Svalbard, European
32
33 Arctic. *Journal of Foraminiferal Research* 272, 101-122.
34
35
36
37 Hald, M., Steinsund, P. I., 1996. Benthic foraminifera and carbonate dissolution in the surface sediments
38
39 of the Barents and Kara Seas. *Berichte zur Polarforschung*, 212, 285-307.
40
41
42 Hammer, Ø., Harper, D.A.T., Ryan, P.D., 2001. PAST: Paleontological statistics software package for
43
44 education and data analysis. *Palaeontologia Electronica*. 41, 9.
45
46
47
48 Harris, C. L., Plueddemann, A. J., Gawarkiewicz, G. G., 1998. Water mass distribution and polar front
49
50 structure in the western Barents Sea. *Journal of Geophysical Research: Oceans*, 103(C2), 2905-2917.
51
52
53
54 Holbourn, A., Henderson, A.S., MacLeod, N., 2013. *Atlas of benthic foraminifera*. John Wiley & Sons. New
55
56 York.
57
58
59
60
61
62
63
64
65

1
2
3
4 IPCC, 2019: Summary for Policymakers. In: IPCC Special Report on the Ocean and Cryosphere in a Changing
5
6
7 Climate [H.-O. Pörtner, D.C. Roberts, V. Masson-Delmotte, P. Zhai, M. Tignor, E. Poloczanska, K.
8
9 Mintenbeck, M. Nicolai, A. Okem, J. Petzold, B. Rama, N. Weyer (eds.)].
10
11
12 Jernas, P., Klitgaard-Kristensen, D., Husum, K., Koç, N., Tverberg, V., Loubere, P., Prins, M., Dijkstra, N.,
13
14
15 Gluchowska, M., 2018. Annual changes in Arctic fjord environment and modern benthic foraminiferal
16
17 fauna: Evidence from Kongsfjorden, Svalbard. *Global and Planetary Change* 163, 119-140.
18
19
20
21 Jorissen, F.J., Wittling, I., 1999. Ecological evidence from live–dead comparisons of benthic foraminiferal
22
23 faunas off Cape Blanc Northwest Africa. *Palaeogeography Palaeoclimatology Palaeoecology* 149, 151-
24
25 170.
26
27
28
29 Koenig, T., Mikolajewicz, U., Jungclaus, J.H., Kroll, A., 2009. Sea ice in the Barents Sea: seasonal to
30
31 interannual variability and climate feedbacks in a global coupled model. *Climate dynamics* 327-8, 1119-
32
33 1138.
34
35
36
37 Koho, K.A., García, R.D., De Stigter, H.C., Epping, E., Koning, E., Kouwenhoven, T.J., Van der Zwaan, G.J.,
38
39 2008. Sedimentary labile organic carbon and pore water redox control on species distribution of benthic
40
41 foraminifera: A case study from Lisbon–Setúbal Canyon southern Portugal. *Progress in Ocean*. 79, 55-82.
42
43
44
45 Korsun, S., Hald, M., 1998. Modern benthic foraminifera off Novaya Zemlya tidewater glaciers, Russian
46
47 Arctic. *Arctic and Alpine Research*, 30(1), 61-77.
48
49
50
51 Lantzsch, H., Hanebuth, T.J., Horry, J., Grave, M., Rebesco, M., Schwenk, T., 2017. Deglacial to Holocene
52
53 history of ice-sheet retreat and bottom current strength on the western Barents Sea shelf. *Quaternary*
54
55 *Science Review*. 173, 40-57.
56
57
58
59
60
61
62
63
64
65

- 1
2
3
4 Levin, L.A., 2005. Ecology of cold seep sediments: Interactions of fauna with flow, chemistry and microbes.
5
6
7 Oceanography and Marine Biology 43, 1-46.
8
9
10 Licari, L.N., Schumacher, S., Wenzhofer, F., Zabel, M., Mackensen, A., 2003. Communities and
11
12 microhabitats of living benthic foraminifera from the tropical east Atlantic: impact of different
13
14 productivity regimes. Journal of Foraminiferal Research 331, 10-31.
15
16
17
18 Lind, S., Ingvaldsen, R.B., Furevik, T., 2018. Arctic warming hotspot in the northern Barents Sea linked to
19
20 declining sea-ice import. Nature Climate Change 87, 634-639.
21
22
23
24 Loeblich, A.R., Tappan, H.N., 1953. Studies of Arctic foraminifera. Smithsonian Miscellaneous Collections,
25
26 121 (7), 1-150.
27
28
29
30 Loeblich, A.R., Tappan, H., 1988. Foraminiferal Genera and Their Classification. Van Nostrand Reinhold Co,
31
32 New York, USA.
33
34
35
36 Loeng, H., 1991. Features of the physical oceanographic conditions of the Barents Sea. Polar Research.
37
38 101, 5-18.
39
40
41 Loeng, H., Ozhigin, V., Ådlandsvik, B., 1997. Water fluxes through the Barents Sea. ICES J. Marine Science.
42
43 543, 310-317.
44
45
46
47 Loubere, P., Jacobsen, B., Kristensen, D.K., Husum, K., Jernas, P., Richaud, M., 2011. The structure of
48
49 benthic environments and the paleochemical record of foraminifera. Deep Sea Research. I 585, 535-545.
50
51
52
53 Lucchi, R.G., Bazzaro, M., Biebow, N., Carbonara, K., Caridi, F., De Vittor, C., Dominiczak, A., Gamboa Sojo,
54
55 V.M., Graziani, S., Kovacevic, V., Krueger, M., Le Gall, C., Mazzini, A., Morigi, C., Musco, M.E., Povea, P.,
56
57 Relitti, F., Ruggiero, L., Rui, L., Sabbatini, A., Sánchez Guillamón, O., Tagliaferro, M., Topchiy, M., Wiberg,
58
59 D., Zoch, D., with the collaboration of the scientific party of the Italian PNRA project DEFROST: Bensi, M.,
60
61
62
63
64
65

1
2
3
4 Deponte, D., Langone, L., Laterza, R., 2016. BURSTER - Bottom Currents in a Stagnant Environment,
5
6 EUROFLEETS-2 Cruise Summary Report. 106. DOI: 10.13140/RG.2.2.24223.36004.

7
8
9 Maslowski, W., Marble, D., Walczowski, W., Schauer, U., Clement, J.L., Semtner, A.J., 2004. On
10 climatological mass, heat, and SAL transports through the Barents Sea and Fram Strait from a pan-Arctic
11
12 coupled ice-ocean model simulation, *Journal of Geophysical Research*, 109, C03032,
13
14 doi:10.1029/2001JC001039.
15
16
17
18

19
20
21 Mau, S., Römer, M., Torres, M.E., Bussmann, I., Pape, T., Damm, E., Geprägs, P., Wintersteller, P., Hsu,
22
23 C.W., Loher, M., Bohrmann, G., 2017. Widespread methane seepage along the continental margin off
24
25 Svalbard-from Bjørnøya to Kongsfjorden. *Scientific reports*, 7(1), 1-13.
26
27
28

29 Murray, J.W., 2006. *Ecology and applications of benthic foraminifera*. Cambridge University Press, UK.
30

31
32 Murray, J. W., Alve, E., 1999. Natural dissolution of modern shallow water benthic foraminifera:
33
34 taphonomic effects on the palaeoecological record. *Palaeogeography, Palaeoclimatology,*
35
36
37 *Palaeoecology*, 146(1-4), 195-209.
38
39

40 Murray, J. W., Alve, E., 2016. Benthic foraminiferal biogeography in NW European fjords: A baseline for
41
42 assessing future change. *Estuarine, Coastal and Shelf Science*, 181, 218-230.
43
44

45
46 Orvik, K.A., Niiler, P., 2002. Major pathways of Atlantic water in the northern North Atlantic and Nordic
47
48 Seas toward Arctic. *Geophysical Research Letters* 2919, 2-1.
49
50

51
52 Peng, G., Steele, M., Bliss, A.C., Meier, W.N., Dickinson, S., 2018. Temporal Means and Variability of Arctic
53
54 Sea Ice Melt and Freeze Season Climate Indicators Using a Satellite Climate Data Record, *Remote Sensing*.
55
56
57 2018, 10, 1328
58
59
60
61
62
63
64
65

1
2
3
4 Pittauerová, D., 2013. Gamma spectrometry for chronology of recent sediments. PhD thesis, Bremen
5
6 University, 213.
7
8
9
10 Pucci, F., Geslin, E., Barras, C., Morigi, C., Sabbatini, A., Negri, A., Jorissen, F.J., 2009. Survival of benthic
11
12 foraminifera under hypoxic conditions: Results of an experimental study using the CellTracker Green
13
14 method. *Marine Pollution Bulletin* 59, 336-351.
15
16
17
18 Rathburn, A.E., Pérez, M.E., Martin, J.B., Day, S.A., Mahn, C., Gieskes, J., J., Ziebis, W., Williams, D., Bahls,
19
20 A., 2003. Relationships between the distribution and stable isotopic composition of living benthic
21
22 foraminifera and cold methane seep biogeochemistry in Monterey Bay, California. *Geochemistry,*
23
24 *Geophysics, Geosystems.* 412.
25
26
27
28
29 Rebesco, M., Liu, Y., Camerlenghi, A., Winsborrow, M., Laberg, J.S., Caburlotto, A., Diviacco, P., Accettella,
30
31 D., Sauli, C., Wardell, N., Tomini, I., 2011. Deglaciation of the western margin of the Barents Sea Ice
32
33 Sheet—A swath bathymetric and sub-bottom seismic study from the Kveithola Trough. *Marine Geology.*
34
35 2791-4, 141-147.
36
37
38
39 Rebesco, M., Özmaral, A., Urgeles, R., Accettella, D., Lucchi, R.G., Rüter, D., Winsborrow, M., Llopart, J.,
40
41 Caburlotto, A., Lantzsch, H., Hanebuth, T.J., 2016. Evolution of a high-latitude sediment drift inside a
42
43 glacially-carved trough based on high-resolution seismic stratigraphy Kveithola, NW Barents Sea.
44
45 *Quaternary Science Review.* 147, 178-193.
46
47
48
49
50 Ritchie, J.C., McHenry, J.R., 1990. Application of radioactive fallout cesium-137 for measuring soil erosion
51
52 and sediment accumulation rates and patterns: A review. *Journal of Environmental Quality* 19, 215-233.
53
54
55
56 Robbins, J.A., Edgington, D.N., 1975. Determination of recent sedimentation rates in Lake Michigan using
57
58 Pb-210 and Cs-137. *Geochimica et Cosmochimica Acta*, 39, 285-304.
59
60
61
62
63
64
65

1
2
3
4 R  ther, D.C., Bjarnad  ttir, L.R., Junntila, J., Husum, K., Rasmussen, T.L., Lucchi, R.G., Andreassen, K., 2012.

5
6
7 Pattern and timing of the northwestern Barents Sea Ice Sheet deglaciation and indications of episodic
8
9 Holocene deposition. *Boreas* 413, 494-512.

10
11
12 Saher, M.H., Kristensen, D.K., Hald, M., Korsun, S., J  rgensen, L.L., 2009. Benthic foraminifera assemblages
13
14 in the Central Barents Sea: an evaluation of combining live and total fauna studies in tracking
15
16 environmental change. *Norwegian Journal of Geology* 89, 149-161
17
18

19
20
21 Saher, M., Kristensen, D.K., Hald, M., Pavlova, O., J  rgensen, L.L., 2012. Changes in distribution of
22
23 calcareous benthic foraminifera in the central Barents Sea between the periods 1965–1992 and 2005–
24
25 2006. *Global and Planet. Change* 98, 81-96.

26
27
28
29 Sakshaug, E., Slagstad, D., 1992 Sea ice and wind: Effects on primary productivity in the Barents Sea.
30
31 *Atmosphere-Ocean* 30, 579-591.

32
33
34
35 Sarnthein, M., Van Kreveld, S., Erlenkeuser, H., Grootes, P.M., Kucera, M., Pflaumann, U., Schulz, M., 2003.
36
37 Centennial-to-millennial-scale periodicities of Holocene climate and sediment injections off the western
38
39 Barents shelf, 75   N. *Boreas* 323, 447-461.

40
41
42
43 Schlitzer, R., 2021. Ocean Data View, <https://odv.awi.de>.

44
45
46 Schr  der, C.J., 1988. Subsurface preservation of agglutinated foraminifera in the northwest Atlantic
47
48 Ocean. *Abhandlungen der geologischen Bundesanstalt* 41, 325-336.
49

50
51
52 Screen, J.A., Simmonds, I., 2010a. The central role of diminishing sea ice in recent Arctic temperature
53
54 amplification. *Nature* 464 (7293), 1334-1337.
55
56
57
58
59
60
61
62
63
64
65

1
2
3
4 Screen, J.A., Simmonds, I., 2010b. Increasing fall-winter energy loss from the Arctic Ocean and its role in
5
6 Arctic temperature amplification. *Geophysical Research Letters* 3716. L16707,
7
8 doi:10.1029/2010GL044136.
9

10
11
12 Seidenkrantz, M. S., 1995. *Cassidulina teretis* Tappan and *Cassidulina neoteretis* new species
13
14 (Foraminifera): stratigraphic markers for deep sea and outer shelf areas. *Journal of Micropalaeontology*,
15
16 14(2), 145-157.
17
18

19
20
21 Sejrup, H. P., Birks, H. J. B., Kristensen, D. K., Madsen, H., 2004. Benthonic foraminiferal distributions and
22
23 quantitative transfer functions for the northwest European continental margin. *Marine*
24
25 *Micropaleontology*, 53(1-2), 197-226.
26
27

28
29 Serreze, M.C., Holland, M.M., Stroeve, J., 2007. Perspectives on the Arctic's shrinking sea-ice cover.
30
31 *Science*, 3155818, 1533-1536.
32
33

34
35 Ślubowska-Woldengen, M., Rasmussen, T.L., Koç, N., Klitgaard-Kristensen, D., Nilsen, F., Solheim, A., 2007.
36
37 Advection of Atlantic Water to the western and northern Svalbard shelf since 17,500 cal yr BP. *Quaternary*
38
39 *Science Review* 263-4, 463-478.
40
41

42
43 Smedsrud, L.H., Esau, I., Ingvaldsen, R.B., Eldevik, T., Haugan, P.M., Li, C., Lien, V.S., Olsen, A., Omar, A.M.,
44
45 Otterå, O.H., Risebrobakken, B., 2013. The role of the Barents Sea in the Arctic climate system. *Review of*
46
47 *Geophysics* 513, 415-449.
48
49

50
51 Solomon, S., Manning, M., Marquis, M., Qin, D., 2007. *Climate change 2007-the physical science basis:*
52
53 *Working group I contribution to the fourth assessment report of the IPCC Vol. 4. Cambridge University*
54
55 *Press, UK.*
56
57
58
59
60
61
62
63
64
65

1
2
3
4 Steinsund, P. I., Polyak, L., Hald, M., Mikhailov, V., Korsun, S., 1994. Distribution of calcareous benthic
5
6
7 foraminifera in recent sediments of the Barents and Kara Sea. Benthic Foraminifera in Surface Sediments
8
9 of the Barents and Kara Seas: Modern and Late Quaternary Application. Ph. D. Thesis, Department of
10
11 Geology, Institute of Biology and Geology, University of Tromsø, Norway.

12
13
14
15 Vinje, T., Kvambekk, Å.S., 1991. Barents Sea drift ice characteristics. Polar Research. 101, 59-68.

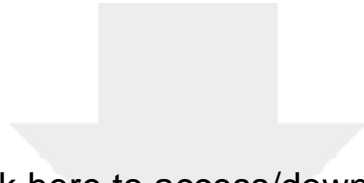
16
17
18 Wassmann, P., Martinez, R., Vernet, M., 1994. Respiration and biochemical composition of sedimenting
19
20
21 organic matter during summer in the Barents Sea. Continental shelf research, 14(1), 79-90.

22
23
24 Wilson, L.J., Hald, M., Godtlielsen, F., 2011. Foraminiferal faunal evidence of twentieth-century Barents
25
26
27 Sea warming. The Holocene 214, 527-537.

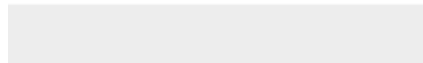
28
29
30 Wollenburg, J. E., Mackensen, A., 1998. Living benthic foraminifers from the central Arctic Ocean: faunal
31
32
33 composition, standing stock and diversity. Marine Micropaleontology. 343-4, 153-185.

34
35
36 Yang, X. Y., Wang, G., Keenlyside, N., 2020. The Arctic sea ice extent change connected to Pacific decadal
37
38
39 variability. Cryosphere 14, 693–708.

40
41
42 Zaborska, A., Carroll, J., Papucci, C., Torricelli, L., Carroll, M. L., Walkusz-Miotk, J., Pempkowiak, J., 2008.
43
44
45 Recent sediment accumulation rates for the Western margin of the Barents Sea. Deep Sea Research. II
46
47
48
49
50
51
52
53
54
55
56
57
58
59
60
61
62
63
64
65



Click here to access/download
RDM Data Profile XML
DataProfile_5639152.xml



Author contributions

R.G.L. and **C.M.** conceived and designed the research. **R.G.L.** PI of BURSTER project. **C.M.** PI of AXED project and conceptualization. **V.M.G.S., F.C., A.S., R.G.L., M.B., V.K., A.T.D., P.P., C.M.** acquired data at sea during the BURSTER cruise. **V.M.G.S.** processed and analysed the dead foraminiferal assemblages and living data $\geq 150 \mu\text{m}$. **V.M., C.M.** and **K.H.** analysed the dead foraminiferal assemblages data. **F.C.** and **A.S.** processed and analysed the living foraminiferal assemblages. **R.G.L.** processed sedimentological data. **M.B., V.K.** processed and analysed oceanographic data. **A.T.D.** processed ^{210}Pb and ^{137}Cs radionuclide measurements. **L.L.** and **A.T.D.** calculated ^{210}Pb -based sedimentation rates. **P.P.** carried out grain size analysis. **V.M.G.S.** wrote the most of the manuscript with contributions from: **C.M.** and **K.H.** dead foraminiferal assemblages, preservation and taphonomic processes; **F.C.** and **A. S.** Living foraminiferal assemblages and modern situation; **R.G.L.** grain size and sedimentological analyses; **M.B.** and **V.K.** oceanographic data and water masses properties; **L.L.** and **A.T.D.** age model and sedimentation rate. All authors discussed the results, the conclusions and reviewed the manuscript.

